THE JOURNAL OF IMMUNOLOGY

Potential Contribution of a Novel Tax Epitope –Specific CD4+ T Cells to Graft-versus-Tax Effect in Adult T Cell Leukemia Patients after Allogeneic Hematopoietic Stem Cell Transplantation

Yotaro Tamai, Atsuhiko Hasegawa, Ayako Takamori, Amane Sasada, Ryuji Tanosaki, Ilseung Choi, Atae Utsunomiya, Yasuhiro Maeda, Yoshihisa Yamano, Tetsuya Eto, Ki-Ryang Koh, Hirohisa Nakamae, Youko Suehiro, Koji Kato, Shigeki Takemoto, Jun Okamura, Naokuni Uike and Mari Kannagi

References	This article cites 50 articles, 30 of which you can access for free at: http://www.jimmunol.org/content/190/8/4382.full#ref-list-1
Subscriptions	Information about subscribing to *The Journal of Immunology* is online at: http://jimmunol.org/subscriptions
Permissions	Submit copyright permission requests at: http://www.aai.org/ji/copyright.html
Email Alerts	Receive free email-alerts when new articles cite this article. Sign up at: http://jimmunol.org/cgi/alerts/etoc

Potential Contribution of a Novel Tax Epitope–Specific CD4⁺ T Cells to Graft-versus-Tax Effect in Adult T Cell Leukemia Patients after Allogeneic Hematopoietic Stem Cell Transplantation

Yotaro Tamai,* Atsuhiko Hasegawa,* Ayako Takamori,* Amane Sasada,*
Ryuji Tanosaki,† Ilseung Choi,‡ Atae Utsunomiya,§ Yasuhiro Maeda,¶ Yoshihisa Yamano,∥
Tetsuya Eto,# Ki-Ryang Koh,** Hirohisa Nakamae,** Youko Suehiro,‡ Koji Kato,††
Shigeki Takemoto,‡‡ Jun Okamura,§§ Naokuni Uike,‡ and Mari Kannagi*

Allogeneic hematopoietic stem cell transplantation (allo-HSCT) is an effective treatment for adult T cell leukemia/lymphoma (ATL) caused by human T cell leukemia virus type 1 (HTLV-1). We previously reported that Tax-specific CD8⁺ cytotoxic T lymphocyte (CTL) contributed to graft-versus-ATL effects in ATL patients after allo-HSCT. However, the role of HTLV-1–specific CD4⁺ T cells in the effects remains unclear. In this study, we showed that Tax-specific CD4⁺ as well as CD8⁺ T cell responses were induced in some ATL patients following allo-HSCT. To further analyze HTLV-1–specific CD4⁺ T cell responses, we identified a novel HLA-DRB1*0101–restricted epitope, Tax155–167, recognized by HTLV-1–specific CD4⁺ Th1-like cells, a major population of HTLV-1–specific CD4⁺ T cell line, which was established from an ATL patient at 180 d after allo-HSCT from an unrelated seronegative donor by in vitro stimulation with HTLV-1–infected cells from the same patient. Costimulation of PBMCs with both the identified epitope (Tax155–167) and known CTL epitope peptides markedly enhanced the expansion of Tax-specific CD8⁺ T cells in PBMCs compared with stimulation with CTL epitope peptide alone in all three HLA-DRB1*0101⁺ patients post–allo-HSCT tested. In addition, direct detection using newly generated HLA-DRB1*0101/Tax155–167 tetramers revealed that Tax155–167-specific CD4⁺ T cells were present in all HTLV-1–infected individuals tested, regardless of HSCT. These results suggest that Tax155–167 may be the dominant epitope recognized by HTLV-1–specific CD4⁺ T cells in HLA-DRB1*0101⁺–infected individuals and that Tax-specific CD4⁺ T cells may augment the graft-versus-Tax effects via efficient induction of Tax-specific CD8⁺ T cell responses. *The Journal of Immunology*, 2013, 190: 4382–4392.

Human T cell leukemia virus type 1 (HTLV-1) is the causative agent of a highly aggressive CD4⁺ T cell malignancy, adult T cell leukemia/lymphoma (ATL) (1, 2). This virus has infected 10–20 million people worldwide, especially in southern Japan, the Caribbean basin, South America, Melanesia, and equatorial Africa (3). Approximately 5% of HTLV-1–seropositive individuals develop ATL, and another 2–3% develop a slow progressive neurologic disorder known as HTLV-1–associated myelopathy/tropical spastic paraparesis (HAM/TSP) or various chronic inflammatory diseases (4). The majority of HTLV-1–infected individuals remain asymptomatic throughout their lives.

ATL is characterized by extremely poor prognosis, mainly because of intrinsic drug resistance to cytotoxic agents. It has been reported that allogeneic hematopoietic stem cell transplantation

(allo-HSCT), but not autologous HSCT, improved the outcome of ATL (5, 6). In previous clinical studies carried out by the ATL allo-HSCT Study Group, the overall survival rate within 3 y after allo-HSCT with reduced intensity conditioning (RIC) was 36% (7). HTLV-1 proviral load became and remained undetectable in some ATL patients with complete remission after allo-HSCT, suggesting that it is an effective treatment for ATL (7–9). In these studies, we reported that donor-derived HTLV-1 Tax-specific CD8⁺ CTLs were induced in some ATL patients who achieved complete remission after allo-HSCT (10). These CTLs were able to lyse recipient–derived HTLV-1–infected T cells in vitro, suggesting potential contributions to graft-versus-leukemia effects. CD8⁺ T cells, especially CTLs, generally play an important role in controlling viral replication in various infections, such as those

*Department of Immunotherapeutics, Tokyo Medical and Dental University, Tokyo 113-8519, Japan; †Clinical Laboratories Division, National Cancer Center Hospital, Tokyo 104-0045, Japan; ‡Department of Hematology, National Kyushu Cancer Center, Fukuoka 811-1395, Japan; §Department of Hematology, Imamura Bun-in Hospital, Kagoshima 890-0064, Japan; ¶Division of Hematology, Department of Internal Medicine, Kinki University School of Medicine, Osaka 589-8511, Japan; ∥Department of Rare Diseases Research, Institute of Medical Science, St. Marianna University Graduate School of Medicine, Kawasaki 216-8512, Japan; #Department of Hematology, Hamanomachi Hospital, Fukuoka 810-8539, Japan; **Department of Hematology, Graduate School of Medicine, Osaka City University, Osaka 545-8585, Japan; ††Department of Medicine and Biosystemic Science, Kyushu University Graduate School of Medical Sciences, Fukuoka 812-8582, Japan; ‡‡Department of Hematology, National Hospital Organization Kumamoto Medical Center, Kumamoto 860-0008, Japan; and §§Institute for Clinical Research, National Kyushu Cancer Center, Fukuoka 811-1395, Japan

involving HIV, hepatitis B virus, and hepatitis C virus. In HTLV-1 infection, HTLV-1–specific CD8$^+$ T cells predominantly recognize the Tax Ag and are believed to contribute to controlling infected cells (11, 12). A high frequency of functional Tax-specific CD8$^+$ T cells can be detected in HAM/TSP patients and some asymptomatic carriers (ACs), whereas most ATL patients and a small population of ACs show severely reduced Tax-specific CD8$^+$ T cell responses (13, 14). The mechanism underlying the suppression of HTLV-1–specific CD8$^+$ T cell responses in these patients has not yet been fully elucidated.

For induction and maintenance of virus-specific CTLs, virus-specific CD4$^+$ Th cell responses are required in many virus infections (15–19). However, there are only a few reports of HTLV-1–specific Th cell responses (20–23), presumably because of their susceptibility to HTLV-1 infection in vivo and in vitro (24). Preferential HTLV-1 infection in HTLV-1–specific CD4$^+$ T cells could be one of the reasons for immune suppression in ATL patients. In addition, it has been reported that a higher frequency of CD4$^+$FOXP3$^+$ regulatory T (Treg) cells is observed in infected individuals compared with uninfected healthy donors. The frequency of Tax$^-$ Treg cells, which are a major population of Treg cells in infected individuals, is negatively correlated with HTLV-1–specific CTL responses (25). HTLV-1 basic leucine zipper factor might also be involved in immune suppression, because HTLV-1 basic leucine zipper was constitutively expressed in infected cells (26) and inhibited the activity of IFN-γ promoters by suppressing NFAT and AP-1 signaling pathways, resulting in the impaired secretion of Th1 cytokines from CD4$^+$ Th cells in a transgenic mouse model (27) These reports suggest that both the dysfunction of HTLV-1–specific CD4$^+$ Th cells and the increased number of uninfected Treg cells might be implicated in the immunosuppression observed in ATL patients. Conversely, in HAM/TSP patients, CD4$^+$ T cells are predominantly found in early active inflammatory spinal cord lesions (28, 29) with spontaneous production of proinflammatory, neurotoxic cytokines, such as IFN-γ and TNF-α (30), suggesting their contributions to the pathogenesis of HAM/TSP. However, the precise roles of HTLV-1–specific CD4$^+$ T cells in HTLV-1 infection remain unclear.

In some ATL patients who achieved complete remission after allo-HSCT, it has been suggested that donor-derived HTLV-1 Tax-specific CTLs may contribute to elimination of ATL cells (graft-versus-Tax effects) (10). We believe that CD4$^+$ T cells also play a critical role in the graft-versus-ATL effects because CD4$^+$ T cells are required for induction and maintenance of optimal CTL responses (15–19). It therefore is important to clarify the role of HTLV-1–specific CD4$^+$ T cells in the effects for understanding HTLV-1–specific T cell immunity in ATL patients after allo-HSCT and for developing new vaccine strategies to prevent recurrence of ATL.

Several studies have reported some HTLV-1–specific CD4$^+$ T cell epitopes restricted by different HLA haplotypes (20–23). The helper functions of these epitopes in HTLV-1–specific CTL responses in HTLV-1–infected individuals have not been well understood. However, Jacobson et al. (20) showed that CD4$^+$ T cells specific for Env gp46 196–209, an epitope restricted by HLA-DQ5 or -DRw16, exhibited a cytotoxic function by directly recognizing HTLV-1–infected cells. This observation raises the possibility that some HTLV-1–specific CD4$^+$ T cells may contribute to the graft-versus-ATL effects through their cytotoxic function in ATL patients after allo-HSCT.

In the current study, we demonstrated that both CD4$^+$ and CD8$^+$ Tax-specific T cell responses were induced in patients after allo-HSCT with RIC for ATL. To further analyze HTLV-1–specific CD4$^+$ T cell responses in ATL patients after allo-HSCT, we determined a novel HLA-DRB1*0101–resricted epitope, Tax155–167, recognized by HTLV-1–specific CD4$^+$ Th1-like cells, a major population of HTLV-1–specific CD4$^+$ T (T4) cell line, which was established from a patient in complete remission following allo-HSCT with RIC. Costimulation with oligopeptides corresponding to the Th1 epitope, Tax155–167, together with a known CTL epitope led to robust expansion of Tax-specific CD8$^+$ T cells in PBMCs from three HLA-DRB1*0101$^+$ patients after allo-HSCT tested. Furthermore, Tax155–167-specific CD4$^+$ T cells were found to be maintained in all HTLV-1–infected HLA-DRB1*0101$^+$ individuals tested, regardless of HSCT, by direct detection with newly generated HLA-DRB1*0101/Tax155–167 tetramers. Our results suggest that Tax155–167 may be a dominant epitope recognized by HTLV-1–specific CD4$^+$ T cells in HTLV-1–infected individuals carrying HLA-DRB1*0101 and that Tax-specific CD4$^+$ T cells may strengthen the graft-versus-ATL effects through efficient induction of Tax-specific CTL responses.

Materials and Methods

Subjects

A total of 18 ATL patients who underwent allo-HSCT with RIC regimen, and one HTLV-1–seronegative (#365) and two seropositive donors (one AC #310 and one HAM/TSP patient #294) carrying HLA-DRB1*0101 donated peripheral blood samples after providing written informed consent. Approximately one-half of these patients received allogeneic peripheral blood stem cell transplantation from HLA-A-, B-, and -DR–identical sibling donors. The other half received allogeneic bone marrow cells from HLA-A–, B–, and DR–identical seronegative unrelated donors (Table I). These patients were the participants of clinical studies organized by the ATL allo-HSCT Study Group, supported by the Ministry of Health, Welfare, and Labor of Japan. This study was also reviewed and approved by the Institutional Ethical Committee Review Board of the Tokyo Medical and Dental University.

Generation of cell lines derived from patients and donors

PBMCs were isolated using Ficoll-Paque PLUS (GE Healthcare, Buckinghamshire, U.K.) density gradient centrifugation and stored in liquid nitrogen in Bambanker stock solution (NIPPON Genetics, Tokyo, Japan) until required. These were used in part to obtain HTLV-1–infected IL-2–dependent T cell lines (ILT) and EBV-transformed lymphoblastoid B cell lines (LCL). ILT-#350 was spontaneously immortalized during long-term culture of PBMCs from patient #350 before allo-HSCT and maintained in RPMI 1640 medium (Life Technologies, Grand Island, NY) containing 20% FCS (Sigma Aldrich, St. Louis, MO) and 30 U/ml recombinant human IL-2 (rhIL-2; Shionogi, Osaka, Japan). LCL-#307, -#341, and -#350 were established by maintaining PBMCs from ATL patients #307, #341, and #350, respectively, after allo-HSCT. These PBMCs were maintained in RPMI 1640 medium containing 20% FCS, following infection with the EBV-containing culture supernatant of the B95-8 cell line, LCL-Kan, derived from a healthy individual was also used.

Synthetic peptides

A total of 18 overlapping peptides, 12- to 25-mer in length, spanning the central region of Tax (residues 103–246) were purchased and used for epitope mapping (Scrum Tokyo, Japan) (Table II). HLA-A*2402–restricted CTL epitopes (Tax301–309, SFHSLHLLF) (10) were used for in vitro stimulation of Tax-specific CTLs (Hokudo, Sapporo, Japan).

GST–Tax fusion protein–based immunoassay

HTLV-1 Tax-specific T cell responses were evaluated using GST–fusion proteins of the N-terminal (residues 1–127), central (residues 113–237), and C-terminal (residues 224–353) regions of HTLV-1 Tax (GST–Tax-A, -B, and -C, respectively) as described previously (13, 31). PBMCs (1 × 10^6 cells/ml) were incubated with or without a mixture of GST–Tax-A, -B, and -C proteins (GST–TaxABC) in 200 μl RPMI 1640 medium supplemented with 10% FCS. After 4 d, the supernatant was collected, and the concentration of IFN-γ in the supernatant was determined using an OptiEIA Human IFN-γ ELISA Kit (BD Biosciences, San Jose, CA). The minimum detectable dose for this assay was determined to be 23.5 pg/ml IFN-γ. CD8$^+$ cells were depleted from PBMCs by negative selection using Dynabeads M-450 CD8 (Invitrogen, Carlsbad, CA), according to the

manufacturer's instructions. For cytokine profiling of a HTLV-1–specific CD4$^+$ T cell line, cells were stimulated with formaldehyde-fixed ILT-#350 for 48 h. Culture supernatant was collected, and various cytokines were measured using a Human Th1/Th2/Th17 Cytokine Kit for a Cytokine Beads Array (BD Biosciences).

Induction of HTLV-1–specific CD4$^+$ T cell line (T4 cells)

PBMCs (1 × 10^6 cells/ml) from patient #350, in complete remission at 180 d after allo-HSCT, were cultured for 2 wk with 100 nM Tax301–309 peptide in 96-well round-bottom tissue culture plate (BD Biosciences) in a final volume of 200 μl RPMI 1640 medium with 20% FCS and 10 U/ml rhIL-2. CD4$^+$ cells were then isolated by negative selection using a Human CD4 T lymphocyte Enrichment Set-DM (BD Biosciences) and maintained in RPMI 1640 medium with 20% FCS and 100 U/ml rhIL-2. Cells (1 × 10^6 cells/ml) were stimulated with formaldehyde-fixed ILT-#350 (2.5 × 10^5 cells/ml) every 2–3 wk. After multiple rounds of stimulation, the resulting CD4$^+$ T cell line was assessed for HTLV-1 specificity by comparing IFN-γ production against ILT-#350 to that against an HTLV-1–negative cell line, LCL-#350.

RT-PCR

Total RNA from cells was isolated using Isogen (Nippon Gene, Tokyo, Japan) and Turbo DNA-free (Life Technologies). First-strand cDNA was prepared from 0.5 μg RNA using ReverTra Ace and Oligo(dT)$_{20}$ primers provided in a ReverTra Ace-α-kit (Toyobo, Osaka, Japan). PCRs were performed in 50 μl reaction mixture containing ReverTra Dash (Toyobo), 0.5 μM of each HTLV-1 pX-specific primer (pX1, 5'-CCA CTT CCC AGG GTT TAG ACA GAT CTT C-3' and pX4, 5'-TTC CTT ATC CCT CGA CTC CCC TCC TTC CCC-3'), and 2 μl cDNA. GAPDH-specific primers (GAPDH5', 5'-ACC ACA GTC CAT GCC ATC AC-3'; GAPDH3', 5'-TCC ACC ACC CTG TTG CTG TA-3') were used as an internal control. The thermal cycling conditions comprised an initial activation step at 94°C for 1 min, followed by 30 cycles of denaturation (98°C, 10 s), annealing (60°C, 2 s), and extension (74°C, 30 s). The PCR amplicons were visualized by ethidium bromide staining following 2% (w/v) agarose gel electrophoresis.

Flow cytometry

For cell surface staining, the following fluorochrome-conjugated mouse anti-human mAbs were used: CD3-FITC (UCHT1; BioLegend, San Diego, CA), CD4-FITC (RPA-T4; BioLegend), CD8-FITC (RPA-T8; BioLegend), and CD8-PE-Cy5 (HIT8a; BD Biosciences, San Jose, CA). For tetramer staining, PE-conjugated HLA-A*0201/Tax11–19, HLA-A*1101/Tax88–96, HLA-A*1101/Tax272–280, and HLA-A*2402/Tax301–309 tetramers were purchased from Medical & Biological Laboratories (Nagoya, Japan). PE-conjugated HLA-DRB1*0101/Tax155–167 tetramer were newly generated through the custom service of Medical & Biological Laboratories. Whole-blood or cultured cells were stained with PE-conjugated Tax/HLA tetramer in conjunction with CD3-FITC and CD8-PE-Cy5 or CD4-PE-

Cy5. For whole-blood samples, RBCs were lysed and fixed in BD FACS lysing solution (BD Biosciences) before washing. Samples were analyzed on a FACSCalibur (BD Biosciences), and data analyses were performed using FlowJo software (Tree Star, Ashland, OR).

Epitope mapping

T4 cells (3 × 10^5 cells/ml) were stimulated with LCL-#350, pulsed with various concentrations of synthetic peptides for 1 h at 37°C, at a responder/stimulator (R/S) ratio of 3. The culture supernatant was collected at 6 h poststimulation, and peptide-specific IFN-γ production from T4 cells was determined by ELISA.

HLA class II restriction assay

T4 cells (5 × 10^5 cells/ml) were cocultured for 6 h with ILT-#350 (1 × 10^5 cells/ml) in the presence or absence of anti-human HLA-DR (10 μg/ml; L243; BioLegend), anti-human HLA-DQ (10 μg/ml; SPVL3; Beckman Coulter, Fullerton, CA), or anti-HLA-ABC (10 μg/ml; W6/32; BioLegend). The IFN-γ in the supernatant was measured by ELISA.

To identify a HLA class II molecule responsible for Ag presentation to T4 cells, Tax155–167 peptide-specific IFN-γ responses were evaluated using various HLA-typed LCLs (LCL-#350, LCL-#341, LCL-#307, and LCL-Kan). These LCLs (1 × 10^5 cells/ml) were pulsed with 100 ng/ml Tax155–167 peptide for 1 h, fixed with 2% formaldehyde, and then cultured with T4 cells (3 × 10^5 cells/ml) for 6 h. The culture supernatant was collected, and IFN-γ in the supernatant was measured by ELISA.

Tetramer-based proliferation assay

PBMCs (1.0 × 10^6 cells/ml) were cultured for 13 or 14 d with or without 100 nM antigenic peptides in the presence of 10 U/ml rhIL-2. Cells were stained with HLA/Tax tetramer-PE, CD3-FITC, and CD8-PE-Cy5 or CD4-PE-Cy5 and then analyzed by flow cytometry.

Statistic analysis

Statistical significance was evaluated with the unpaired t test using Graphpad Prism 5 (Graphpad Software, La Jolla, CA). In all cases, two-tailed p values <0.05 were considered significant.

Results

Tax-specific T cell responses in ATL patients who received allo-HSCT with RIC

We previously reported that Tax-specific CD8$^+$ T cells were induced in some ATL patients after allo-HSCT with RIC from HLA-identical sibling donors (10). In this study, we examined the Tax-specific T cell response in a larger number of ATL patients who received allo-HSCT with RIC. Table I provides a summary of the

Table I. Clinical information and summary for Tax-specific CD8$^+$ T cells in 18 ATL patients at 180 d post–allo-HSCT with RIC

ID (Age, Sex)	ATL Subtype	Type of Donor	Donor-HLA	Donor HTLV-1 Sero Status	Chimerism (%)^a	Tetramer (%)^b	Proviral Load^c
239 (55, M)	Lymphoma	r-PB	A 26/33, DR 4/13	(−)	<5	NT	0.1
241 (61, F)	Acute	r-PB	A 2/26, DR 10/18	(−)	<5	0.00	0.1
247 (52, F)	Lymphoma	r-PB	A 24/−, DR 9/15	(−)	<5	0.07	0.1
270 (57, M)	Lymphoma	r-PB	A 24/33, DR 13/15	(−)	<5	0.00	0.0
300 (53, F)	Lymphoma	r-PB	A 24/26, DR 4/15	(+)	<5	1.34	4.8
301 (57, F)	Acute	ur-BM	A 24/33, DR 13/15	(−)	<5	0.72	0.0
307 (68, M)	Acute	r-PB	A 2/11, DR 14/15	(+)	<5	0.10	5.4
317 (60, M)	Acute	ur-BM	A 2/24, DR 14/15	(−)	<5	0.92	0.0
328 (62, M)	Acute	ur-BM	A 11/24, DR 8/9	(−)	<5	0.75	NT
340 (50, M)	Acute	r-PB	A 2/24, DR 4/8	(−)	<5	1.40	0.7
341 (61, F)	Acute	ur-BM	A 24/33, DR 1/15	(−)	<5	0.45	0.1
344 (58, M)	Lymphoma	ur-BM	A 2/24, DR 4/−	(−)	<5	0.44	0.0
349 (53, M)	Acute	r-PB	A 24/−, DR 8/15	(+)	<5	0.00	0.0
350 (60, F)	Acute	ur-BM	A 24/26, DR 1/14	(−)	<5	0.59	0.6
351 (57, F)	Acute	ur-BM	A 24/26, DR 9/12	(−)	<5	0.45	0.0
358 (63, F)	Lymphoma	r-PB	A 2/11, DR 4/14	(−)	<5	0.42	0.0
352 (61, M)	Acute	ur-BM	A 11/26, DR 8/15	(−)	<5	0.14	0.0
364 (52, M)	Acute	r-PB	A 24/26, DR 1/−	(−)	<5	0.11	0.0

^{a}Indicates percentage of recipient-derived T cell chimerism.
^{b}Indicates percentage of tetramer$^+$ cells among CD8$^+$ T cells in PBMCs.
^{c}Indicates copy number per 1000 PBMCs.
F, Female; M, male; NT, not tested; r-PB, related donor-derived peripheral blood stem cell; ur-BM, unrelated donor-derived bone marrow cell.

results of Tax-specific CD8$^+$ T cell detection by flow cytometry, using the Tax/HLA tetramers, in the peripheral blood of 18 ATL patients at 180 d after allo-HSCT, together with clinical information. During this period, all patients achieved a complete chimera state consisting of >95% of donor-derived hematopoietic cells. By using four available tetramers (HLA-A*0201/Tax11–19, HLA-A*2402/Tax301–309, HLA-A*1101/Tax88–96, and HLA-A*1101/Tax272–280), Tax-specific CD8$^+$ T cells were found in 14 patients. Because the donors were uninfected individuals in the majority of cases (Table I), induction of the Tax-specific donor-derived CD8$^+$ T cells in recipients indicated the presence of newly occurring immune responses against HTLV-1 in the recipients. This evidence strengthens our previous observation (10, 32).

We also used a GST–Tax fusion protein-based assay to evaluate Tax-specific T cell responses. The tetramer-based assay was limited to four kinds of epitopes and restricted by three HLA alleles but did not detect T cells directed to other epitopes or HLAs. The GST–Tax fusion protein-based assay can detect both CD4$^+$ and CD8$^+$ T cell responses, irrespective of HLA types. However, this sensitivity is not as good as single-cell analysis by flow cytometry (31). As shown in Fig. 1A, there was a wide variation in the IFN-γ responses to the Tax protein in the PBMCs among the 16 patients tested. In five patients (#247, #270, #328, #340, and #349), IFN-γ production of PBMCs against GST–TaxABC proteins was very low or not specific for the Tax protein. PBMCs from the other 11 patients (#239, #241, #301, #317, #341, #344, #350, #351, #352,

#358, and #364) produced higher amounts of IFN-γ in response to GST–TaxABC proteins compared with GST. However, the levels of IFN-γ production varied among the patients.

We also evaluated the extent to which Tax-specific CD4$^+$ T cells were responsible for IFN-γ in the GST–Tax-based immunoassay system. We used PBMCs from patients #350 and #341, who showed high Tax-specific T cell responses. CD8$^+$ cell–depleted PBMCs from patient #350 and #341 showed a reduced but still significant level of Tax-specific IFN-γ–producing response compared with whole PBMCs (Fig. 1B). These results indicate that not only CD8$^+$ but also CD4$^+$ T cells against Tax are present in the peripheral blood from patient #350 and #341 after allo-HSCT with RIC.

Induction of an HTLV-1–specific CD4$^+$ T cell line from patient #350

We next attempted to induce HTLV-1–specific CD4$^+$ T cells from the PBMCs of patient #350 at 180 d after allo-HSCT, using an HTLV-1–infected T cell line (ILT-#350) as APCs. Freshly isolated PBMCs were stimulated for 2 wk with Tax301–309, a dominant CTL epitope presented by HLA-A*2402, to eliminate HTLV-1–infected cells, which potentially existed in PBMCs. The CD4$^+$ cells were then isolated from the cultured cells and stimulated with formaldehyde-fixed ILT-#350 every 2–3 wk. The established cell line was found to be a CD4$^+$ T cell line (designated as T4 cells thereafter) because cells expressed CD3 and CD4 but not CD8
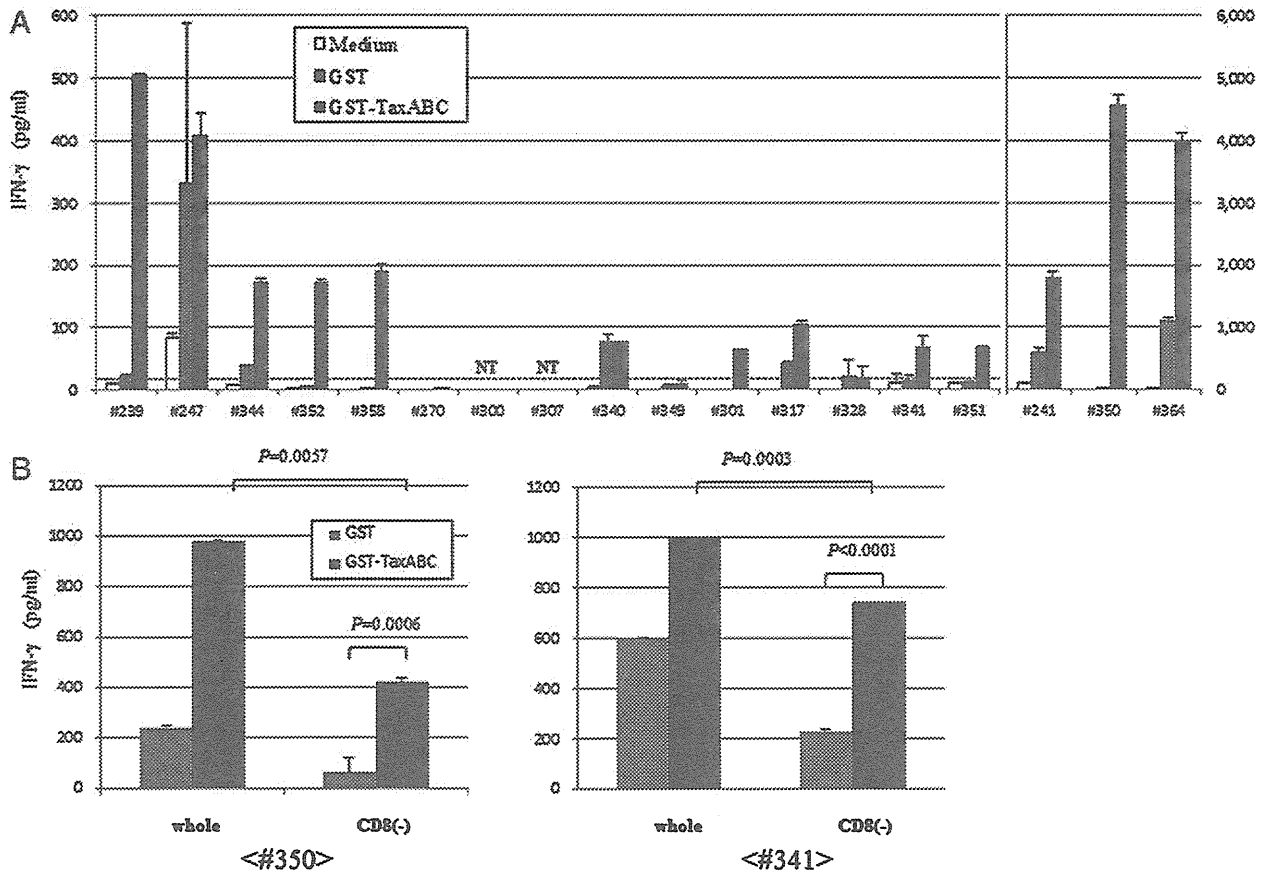

FIGURE 1. Diversity of Tax-specific T cell responses in ATL patients who received allo-HSCT with RIC. (A and B) PBMCs from 18 ATL patients at 180 d after allo-HSCT (A) or whole and CD8$^+$ cell–depleted PBMCs from two patients at 540 d after allo-HSCT (#350 and #341) (B) were cultured for 4 d in the absence (open square) or presence of GST (gray square), or GST–Tax (black square) proteins. The concentration of IFN-γ in the supernatant was determined by ELISA. The y-axis on the right side indicates the results from three patients (#241, #350, and #364). The dotted horizontal line indicates the detection limit (23.5 pg/ml). The error bars represent SD of duplicated wells. The representative result of two independent experiments is shown in (B).

(Fig. 2A). Because HTLV-1 has been shown to preferentially infect CD4$^+$ T cells in vivo and in vitro (24), we examined HTLV-1 expression in T4 cells by RT-PCR (Fig. 2B). As expected, the T4 cells did not express HTLV-1 Tax, indicating that the cells were not infected with HTLV-1. We assessed expression of various cytokines in T4 cells (Fig. 2C). The T4 cells were stimulated with formaldehyde-fixed ILT-#350 or LCL-#350. The cells produced large amounts of IFN-γ and TNF-α and small amounts of IL-2, IL-4, and IL-10 in response to ILT-#350 but not against LCL-#350. IL-6 and IL-17A were not detected in the culture supernatant. These data indicate that T4 cells are mainly HTLV-1–specific CD4$^+$ Th1-like cells but contain minor populations to produce Th2 cytokines.

Determination of the minimum epitope recognized by T4 cells

Freshly isolated PBMCs in the patient #350 produced IFN-γ in response to GST–Tax (Fig. 1A). We expected that the epitope recognized by the T4 cells should be present in the Tax protein. We therefore examined whether the T4 line responded to Tax using LCL-#350 pulsed with GST–Tax proteins as APCs. As shown in Fig. 3A, the T4 cells produced significantly higher amounts of IFN-γ in response to GST–TaxABC and GST–Tax-B (residues 113–237) (31) but not GST–Tax-A (residues 1–127) (31) and -C (residues 224–353 (31), when compared with the GST control protein, indicating that the T4 cells recognized the central region (residues 113–237) of the Tax Ag. We next synthesized eight overlapping 25-mer peptides spanning the central region of Tax (residues 103–246) and analyzed their abilities to stimulate T4 cells (Table II). The cell line produced high amounts of IFN-γ only when stimulated with Tax154–178 (Fig. 3B). We then prepared four overlapping 15-mer peptides, covering residues 154–178 of Tax, to examine the IFN-γ responses of the T4 cells (Table II). Both Tax151–165 and Tax156–170-stimulated cells to induce IFN-γ responses but not at a comparable level to Tax154–178 (Fig. 3C). These results suggest that the epitope recognized by T4 cells might be present in the N-terminal half of Tax154–178. We therefore stimulated the cells with Tax154–168, Tax155–169, or Tax156–170.

The cells showed higher IFN-γ responses against Tax154–168 and Tax155–169 than Tax156–170, indicating that the minimum epitope might be within residues 155–168 of Tax (Fig. 3D). To identify the minimum epitope recognized by T4 cells, we next synthesized three overlapping peptides of 12- to 14-mer lengths beginning at residue 155 of Tax (Table II). Tax155–167 induced IFN-γ responses in cells at a similar level to Tax155–169 and Tax155–168, although Tax155–166 did not (Fig. 3E). Moreover, IFN-γ production of cells in response to various concentrations of Tax155–167 was comparable to that against Tax155–169 and Tax155–168 (Fig. 3F). These data clearly show that the minimum epitope recognized by the T4 cells is Tax155–167.

HLA-DRB1*0101 restriction of Tax-specific T4 cells

To analyze HLA class II molecules involved in the presentation of the minimum epitope, T4 cells were stimulated with ILT-#350 in the presence or absence of anti–HLA-DR, -DQ, and anti-HLA class I blocking Abs. As shown in Fig. 4A, the addition of an anti–HLA-DR blocking Ab abrogated IFN-γ responses of the T4 cells against ILT#-350, indicating that the epitope was HLA-DR restricted.

We further investigated the HLA-DR alleles responsible for the presentation of the minimum epitope by using four HLA-typed LCLs displaying different HLA-DRs. As shown in Fig. 4B, the T4 cells responded by producing IFN-γ when Tax155–167 was presented by autologous LCL-#350 (DR1/14) and allogeneic LCL-#341 (DR1/15). These results clearly indicate that this epitope is presented by HLA-DRB1*0101 on APCs. We searched for a known HLA-DRB1*0101 motif in the identified epitope Tax155–167 and found that this epitope contained the HLA-DRB1*0101 motif (Fig. 4C) (33).

Enhancement of Tax-specific CD8$^+$ T cell expansion by Tax155–167-specific CD4$^+$ T cell help

As T4 cells were established from PBMCs of an HTLV-1–infected patient #350, it is suggested that Tax155–167-specific CD4$^+$ T cells may be maintained in the HLA-DRB1*0101$^+$ patient #350.
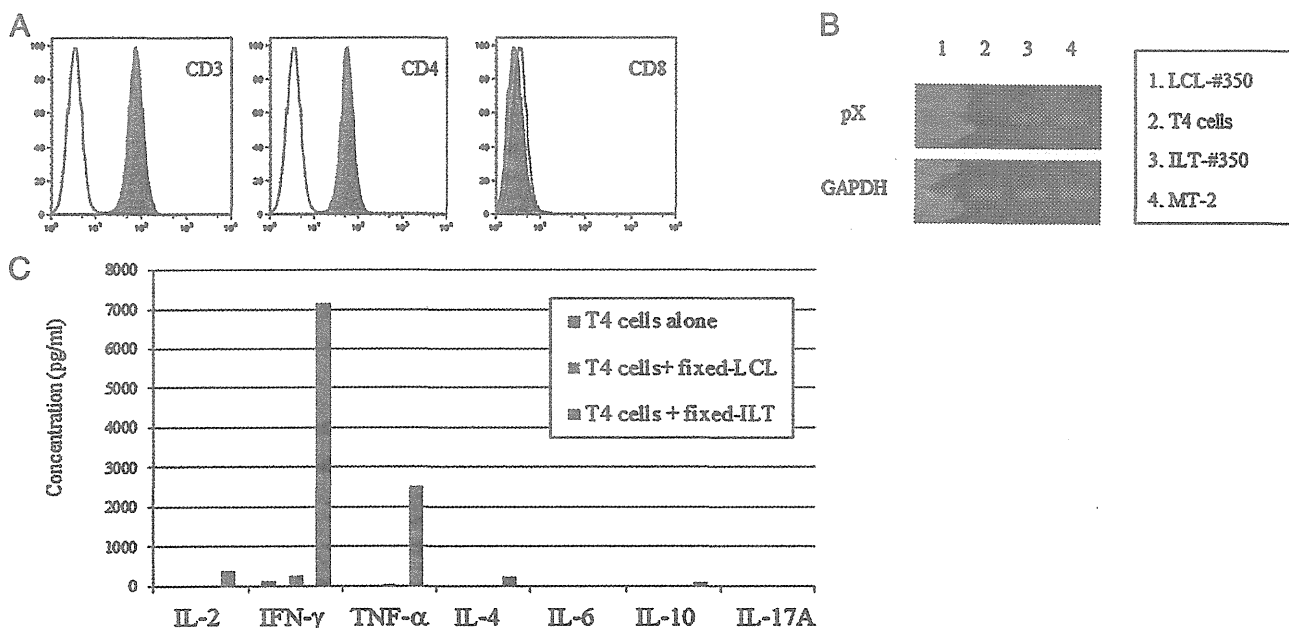

FIGURE 2. Phenotype and function of CD4$^+$ T cell line (T4) generated from patient #350. (A) Cell surface phenotype of T4 cells was analyzed by flow cytometry. (B) Total RNA was extracted from LCL-#350 (*lane 1*), T4 cells (*lane 2*), ILT-#350 (*lane 3*), and MT-2 (*lane 4*). Tax mRNA expression for each cell type was analyzed by RT-PCR. GAPDH was used as an internal control. (C) T4 cells were stimulated for 24 h with or without formaldehyde-fixed ILT-#350 or LCL-#350 cells. The concentration of indicated cytokines in the supernatants was measured using a cytometric bead array system.
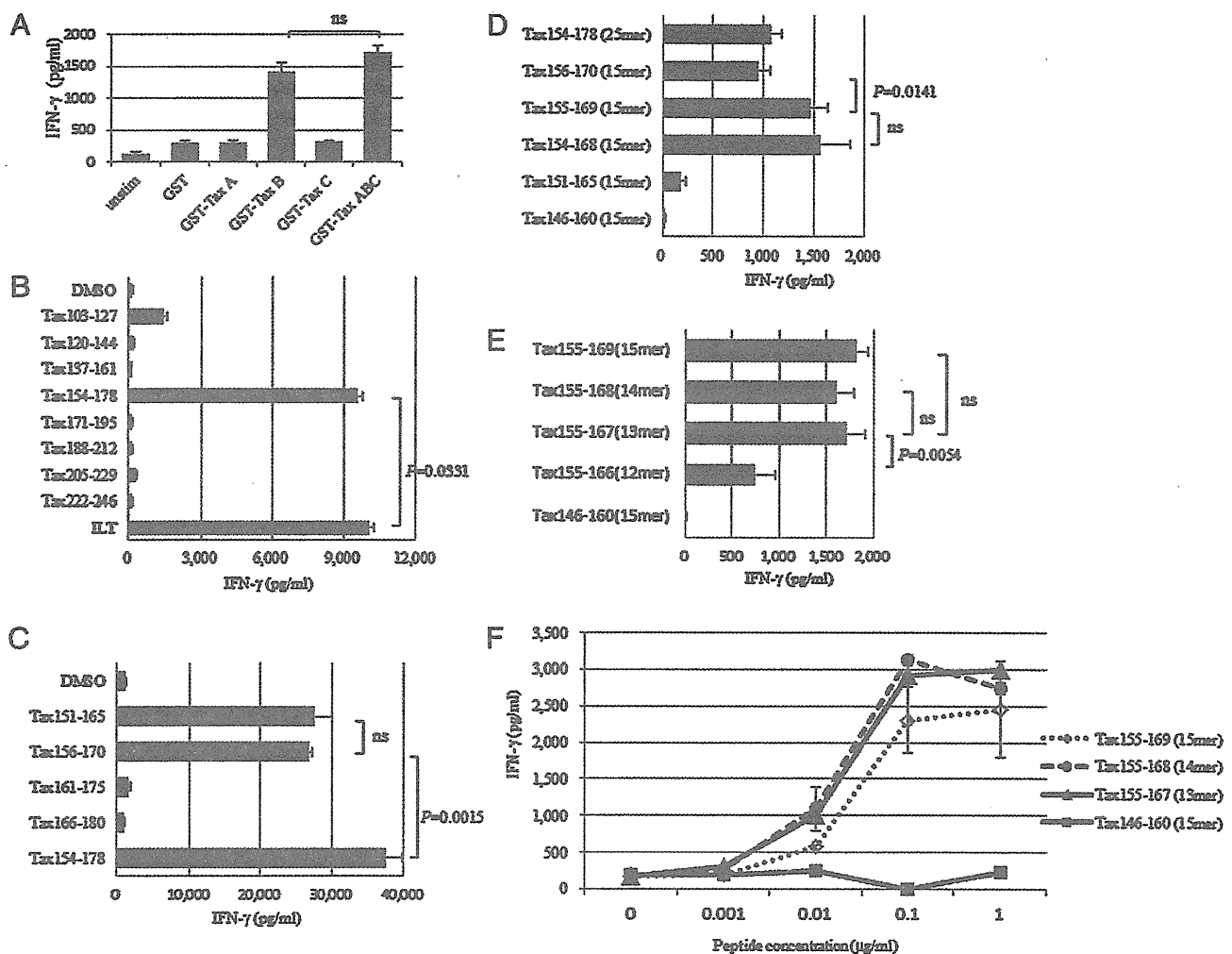
FIGURE 3. Identification of the dominant Tax-derived epitope recognized by established T4 cells. (A) Donor-derived LCL-#350 was pulsed with GST, GST–Tax-A, GST–Tax-B, GST–Tax-C, or a mixture of GST–Tax-A, -B, and -C (GST–TaxABC) for 24 h and then cocultured for 24 h with the T4 cells at a responder/stimulator (R/S) ratio of 3. IFN-γ production from T4 cells was analyzed by ELISA. (B and C) LCL-#350 was pulsed with the indicated overlapping 25-mer-long (B) or 15-mer-long (C) synthetic peptides (10 μg/ml) within the Tax-B region for 1 h. Formaldehyde-fixed ILT-#350 cells were cocultured with T4 cells for 6 h. IFN-γ in the supernatant was measured by ELISA. (D and E) IFN-γ responses of T4 cells were assessed using the indicated overlapping 12- to 25-mer-long synthetic peptides (100 ng/ml). (F) IFN-γ responses of T4 cells against indicated concentrations of 13- to 15-mer-long peptides were assessed as in (B) and (C). (A–F) Results are representative of two or three independent experiments. The error bars represent SD of triplicate wells. Statistical significance was analyzed by the unpaired t test.

We therefore evaluated the helper function of Tax155–167-specific CD4+ T cells on the expansion of dominant Tax-specific CTLs in fresh PBMCs of the patient #350. Freshly isolated PBMCs from patient #350 (A24/26, DR1/14) at 540 d after allo-HSCT were stimulated for 13 d with the HLA-A24–restricted CTL epitope peptide (Tax301–309) in the presence or absence of the HLA-DRB1*0101–restricted CD4+ Th epitope peptide (Tax155–167), and Tax-specific CD8+ T cell expansion was evaluated using the HLA-A*2402/Tax301–309 tetramer. As shown in Fig. 5, Tax301–309-specific CD8+ T cells proliferated to 9.26% of CD8+ T cells when stimulated with Tax301–309 alone. Surprisingly, a highly elevated frequency (62.3%) of tetramer-binding CD8+ T cells was detected by in vitro costimulation with Tax301–309 and Tax155–167, suggesting the presence of Tax155–167-specific CD4+ Th cells in patient #350.

We examined whether Tax155–167-specific CD4+ T cells existed and functioned as helper cells in the other two HTLV-1–infected HLA-DRB1*0101+ patients after allo-HSCT (day 360 for patient #341 and day180 for #364). These patients had detectable

levels of HLA-A*2402/Tax301–309 tetramer-binding CD8+ T cells in the peripheral blood (Fig. 5). In patients #341 and #364, the tetramer-binding cells expanded to 7.7 and 0.849% of CD8+ T cells at 13 d of culture when stimulated with the CTL epitope peptide, Tax301–309, alone. Costimulation of PBMCs with both peptides Tax155–167 and Tax301–309 led to a vigorous proliferation of tetramer-binding CD8+ T cells (59.6% for patient #341 and 15.5% for patient #364) as observed in patient #350 (Fig. 5). These results indicate that Tax155–167-specific CD4+ T cells may be present and contribute to enhancing CD8+ T cell responses in HTLV-1–infected HLA-DRB1*0101+ individuals after allo-HSCT.

*Tax155–167-specific CD4+ T cells were maintained in HTLV-1–infected HLA-DRB1*0101+ individuals*

We next generated the HLA-DRB1*0101/Tax155–167 tetramer to directly detect Tax155–167-specific CD4+ T cells and examined the presence of Tax155–167-specific CD4+ T cells in the PBMCs freshly isolated from two HLA-DRB1*0101+ patients after allo-HSCT (day 180 for patient #350 and day 360 for patient #364).

Table II. Synthetic oligopeptides used in this study

```
Peptide                                    Sequence

Tax103-127  P S F L Q A M R K Y S P F R N G Y M E P T L G Q H
Tax120-144  M E P T L G Q H L P T L S F P D P G L R P Q N L Y
Tax137-161  G L R P Q N L Y T L W G G S V V C M Y L Y Q L S P
Tax154-178  M Y L Y Q L S P P I T W P L L P H V I F C H P G Q
Tax171-195  V I F C H P G Q L G A F L T N V P Y K R I E E L L
Tax188-212  Y K R I E E L L Y K I S L T T G A L I I L P E D C
Tax205-229  L I I L P E D C L P T T L F Q P A R A P V T L T A
Tax222-246  R A P V T L T A W Q N G L L P F H S T L T T P G I
Tax146-160        L W G G S V V C M Y L Y Q L S
Tax151-165              V V C M Y L Y Q L S P P I T W
Tax154-168                  M Y L Y Q L S P P I T W P L L
Tax155-169                    Y L Y Q L S P P I T W P L L P
Tax156-170                      L Y Q L S P P I T W P L L P H
Tax161-175                              P P I T W P L L P H V I F C H
Tax166-180                                  P L L P H V I F C H P G Q L G
Tax155-168                    Y L Y Q L S P P I T W P L L
Tax155-167                    Y L Y Q L S P P I T W P L
Tax155-166                    Y L Y Q L S P P I T W P
```

Tax155–167-specific CD4$^+$ T cells were detected ex vivo in the patient #350 (0.11%) and proliferated to 11.6% among CD4$^+$ T cells at 13 d poststimulation with Tax155–167 peptide. In the patient #364, tetramer-binding CD4$^+$ T cells were undetectable in fresh PBMCs but expanded to 0.37% by in vitro stimulation with Tax155–167 peptide (Fig. 6A). In an HLA-DRB1*0101$^+$–sero-negative donor #365, Tax155–167-specific CD4$^+$ T cells were not found in fresh PBMCs and did not become detectable at 13 d after stimulation with Tax155–167 peptide (Fig. 6A). This result indicates that Tax155–167-specific CD4$^+$ T cells are maintained and possesses the abilities to proliferate in response to HTLV-1 Tax in these patients.

We further examined whether Tax155–167-specific CD4$^+$ T cells existed in two HTLV-1–infected individuals carrying HLA-DRB1*0101, an AC #310 and a HAM/TSP patient #294, and detected 0.18 and 0.31% of tetramer-binding cells in peripheral CD4$^+$ T cells, respectively (Fig. 6B). These results suggest that Tax155–167-specific CD4$^+$ T cells are maintained in HTLV-1–infected individuals expressing an HLA-DRB1*0101 allele, regardless of HSCT.

Discussion

In this study, we demonstrated Tax-specific CD4$^+$ T cell responses in some ATL patients post–allo-HSCT and identified a novel HLA-DRB1*0101–restricted CD4 T cell epitope, Tax155–167, which was recognized by HTLV-1–specific CD4$^+$ T cells and consequently led to robust Tax-specific CD8$^+$ T cell expansion. We also found that Tax155–167-specific CD4$^+$ T cells existed in all HTLV-1–infected HLA-DRB1*0101$^+$ individuals tested, regardless of HSCT, by newly generated HLA-DRB1*0101/Tax155–167 tetramers. These results suggest that Tax155–167 might be a dominant epitope recognized by HTLV-1–specific CD4$^+$ T cells
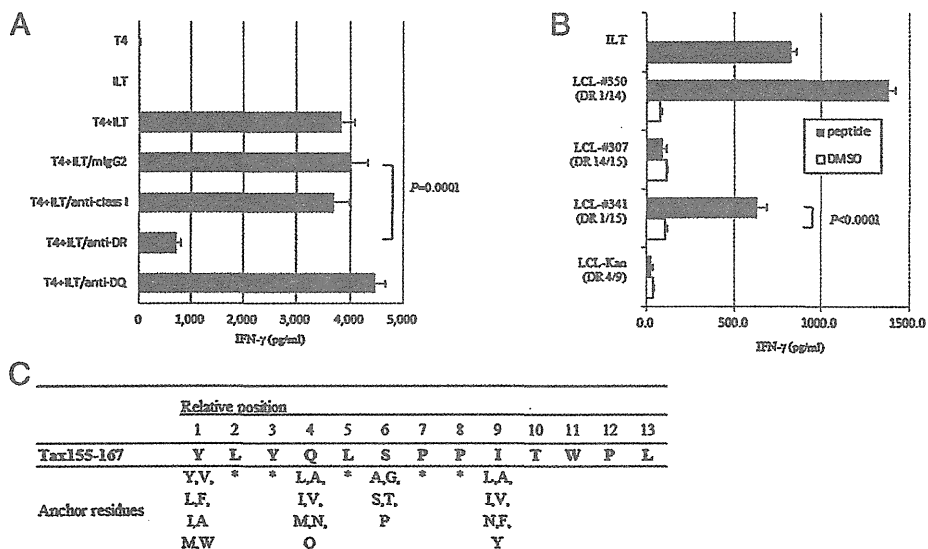

FIGURE 4. HLA-DRB1*0101 restriction of Tax155–167 recognition by established T4 cells. (A) T4 cells were cocultured for 6 h with ILT-#350 in the presence or absence of the following blocking Abs (10 μg/ml): anti-human HLA-DR; anti-human HLA-DQ; anti–HLA-class I; or isotype control. IFN-γ production from T4 cells was measured by ELISA. (B) The T4 cells were cocultured for 6 h with autologous (#350) or allogeneic (#307, #341, and Kan) LCLs pulsed with (closed bar) or without (open bar) Tax155–167 for 1 h or with recipient-derived ILT-#350. The HLA-DR alleles of each LCL line are indicated in parentheses. IFN-γ production of T4 cells was assessed by ELISA. (A and B) Representative data of three independent experiments are shown. The error bars represent SD of triplicate wells. Statistical significance was analyzed by the unpaired t test. (C) The amino acid sequence between residues 155 and 167 of Tax contained a putative HLA-DRB1*0101 anchor motif (33).

FIGURE 5. Augmentation of Tax-specific CD8+ T cell expansion by costimulation with CTL epitope and Tax155–167 peptides. PBMCs from HLA-DRB1*0101– and HLA-A24–expressing ATL patients (#350, #364, and #341) who underwent allo-HSCT with RIC were cultured for 13 d in the presence of DMSO, 100 nM CTL epitope (Tax301–309), or a mixture of Tax301–309 (100 nM) and Tax155–167 (100 nM) peptides. Data indicate percentages of HLA-A*2402/Tax301–309 tetramer+ cells among CD3+CD8+ T cells. Fresh indicates frequency of HLA-A*2402/Tax301–309 tetramer+CD8+ T cells detected in fresh peripheral blood.
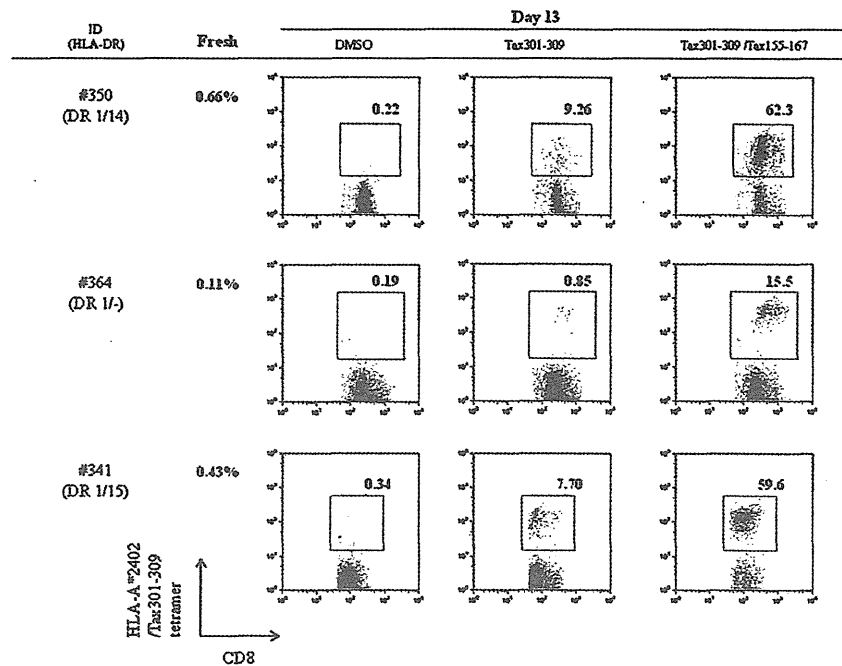
in HTLV-1–infected individuals expressing HLA-DRB1*0101 and that Tax-specific CD4+ T cells might efficiently induce HTLV-1–specific CTL expansion to strengthen the graft-versus-ATL effects in ATL patients after allo-HSCT.

In HTLV-1 infection, analysis of virus-specific CD4+ T cell responses appears to be limited because CD4+ T cells are preferentially infected with HTLV-1 (24, 34, 35), and HTLV-1 Ags are produced from infected cells at a few hours postculture (34, 36). In this study, we used blood samples from 18 ATL patients after allo-HSCT with RIC and from HLA identical–related or unrelated donors and found that these recipients had undetectable or very low proviral loads (Table I), as previously shown (7–9). We previously reported that Tax-specific CTLs were induced in some patients with complete remission after allo-HSCT for ATL and

might contribute to the graft-versus-leukemia effect (10). In the current study, Tax-specific T cell responses or tetramer-binding CD8+ T cells were detected in 68.8% (11 of 16) or 82.4% (14 of 17) of patients tested, respectively (Fig. 1A, Table I). In addition, helper function of Tax-specific CD4+ T cells to enhance Tax-specific CD8+ T cell expansion was observed in PBMCs from all three HLA-DRB1*0101+ patients tested (Fig. 5). These data suggest that both CD8+ and CD4+ Tax-specific T cell responses might contribute to elimination of remaining leukemic and/or infected cells in some patients having T cell responses against Tax. However, given the fact that not all ATL patients who achieved complete remission after allo-HSCT had Tax-specific CD8+ T cells, graft-versus-host reaction may mainly contribute to achieve complete remission after allo-HSCT. It is of note that Tax-specific
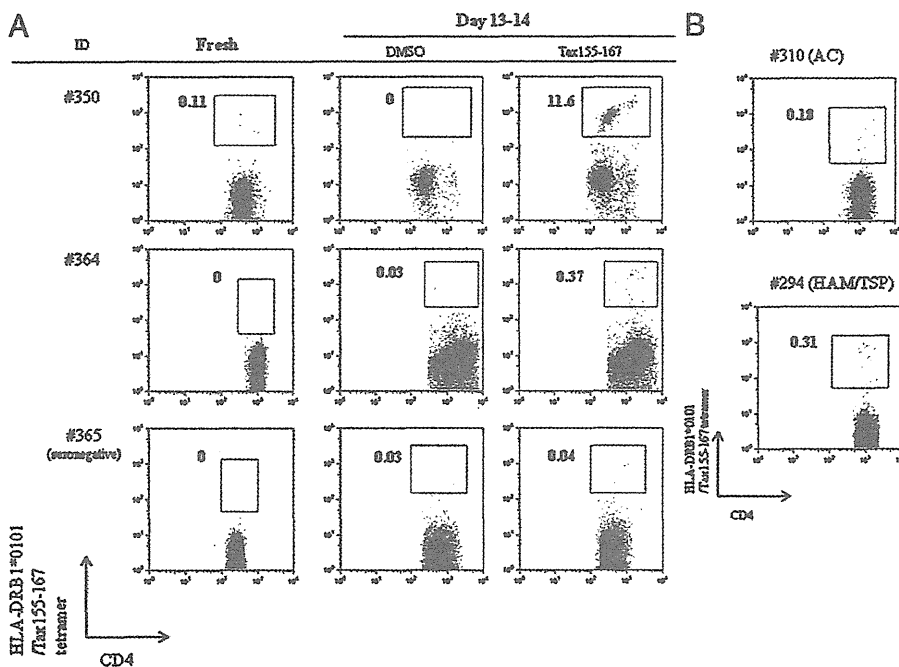

FIGURE 6. Detection of Tax155–167-specific CD4+ T cells in HTLV-1–infected HLA-DRB1*0101+ individuals. (A) In two ATL patients after allo-HSCT (#350 and #364) and an HLA-DRB1*0101+–seronegative donor (#365), frequency of HLA-DRB1*0101/Tax155–167 tetramer-binding CD4+ T cells was analyzed in fresh PBMCs and PBMCs cultured for 13–14 d in the presence of Tax155–167 (100 nM) peptide. Data indicate percentages of tetramer+ cells in CD3+CD4+ T cells. (B) Frequency of HLA-DRB1*0101/Tax155–167 tetramer-binding CD4+ T cells in fresh PBMCs from an AC #310 and an HAM/TSP patient #294 was analyzed. Data indicate percentages of tetramer+ cells in CD3+CD4+ T cells.

T cell responses were detected in 57.1% (four of seven) or 87.5% (seven of eight) of the patients after allo-HSCT with RIC from HTLV-1–seronegative sibling or unrelated donors, respectively. A Tax-specific T cell response was not detected in three patients who underwent allo-HSCT from seropositive donors (Fig. 1, Table I).

It has been proposed that CTLs are the main effector cells against many pathogenic viruses, including HTLV-1. To date, many CTL epitopes recognized by HTLV-1–specific CTLs have been identified, some of which are thought to be the candidates of peptide-based T cell immunotherapy (10, 20, 32, 37–40). CD4$^+$ T cells have also been known to be critical for induction and maintenance of Ag-specific CD8$^+$ T cells (15–19). With respect to HTLV-1 infection, there are several reports identifying HLA-DRB1*0101–restricted epitopes recognized by CD4$^+$ T cells against Env or Tax (Env380–394 (21), Env436–450, Env451–465, Env456–470 (23), and Tax191–205 (22)), which were established by stimulating PBMCs from uninfected or infected individuals with synthetic peptides. In this study, for determination of an epitope recognized by HTLV-1–specific CD4$^+$ T cells, we established an HTLV-1–specific CD4$^+$ T cell line from the patient #350 at 180 d after allo-HSCT by several stimulations with an HTLV-1 Ags-expressing T cell line (ILT-#350) from the same patient. In addition, we found that Tax155–167-specific CD4$^+$ T cells were present in peripheral blood from patient #350 at 180 and 540 d after all-HSCT, indicating that the epitope, Tax155–167, identified in this study is naturally presented on HTLV-1–infected cells and predominantly recognized by HTLV-1–specific CD4$^+$ Th cells in the patient #350 at least within 540 d after allo-HSCT. Another HLA-DRB1*0101–restricted Tax epitope, Tax191–205, has been reported previously (22). In this study, the amino acid sequence within this region was revealed to be conserved in the infected T cell line, ILT-#350 established from the patient #350 (data not shown), indicating that Tax191–205 can be presented on APCs and Tax191–205-specific CD4$^+$ T cells may be induced in patient #350. However, Tax155–167-specific but not Tax191–205-specific CD4$^+$ T cells were revealed to predominantly appear in the HTLV-1–specific T4 cell line, established from PBMCs in the patient #350 at 180 d after allo-HSCT. This suggests that in the case of patient #350 at 180 d after allo-HSCT, Tax191–205-specific CD4$^+$ T cells may not be the most frequent population among HTLV-1–specific CD4$^+$ T cells.

It has been known that Ag-specific effector and memory CD4$^+$ T cells are typically present at much lower frequencies than their CD8$^+$ counterparts and that MHC class II tetramer might have a weak TCR–MHC affinity (41). Although this limited affinity of MHC class II tetramer might preclude detection of Ag-specific low-affinity CD4$^+$ T cells, the low-affinity CD4$^+$ T cells, below detection with MHC class II tetramers, were also proved to be critical effectors in Ag-specific responses (42). In the current study, MHC class II tetramer analysis revealed that Tax155–167-specific CD4$^+$ T cells were present in HLA-DRB1*0101$^+$ HTLV-1–infected individuals: two ATL patients after allo-HSCT (day 180 for #350 and day 360 for #364), an AC #310, and a HAM/TSP patient #294 (Fig. 6). Because of a shortage of blood sample from patient #341, we could not perform the direct detection for Tax155–167-specific CD4$^+$ T cells by the MHC class II tetramers. However, enhanced expansion of Tax301–309-specific CD8$^+$ T cells was observed in patient #341 at 360 d after allo-HSCT when PBMCs were stimulated with Tax301–309 in the presence of Tax155–167 (Fig. 5). So far, Tax155–167-specific CD4$^+$ T cells were detected in fresh and/or Tax155–167-stimulated PBMCs of all HTLV-1–infected HLA-DRB1*0101$^+$ individuals tested, although their frequencies were various. These results suggest that Tax155–167 may be the dominant epitope recognized by Tax-

specific CD4$^+$ T cells in HTLV-1–infected HLA-DRB1*0101$^+$ individuals. In ATL patients after HSCT, the donor-derived T cells reconstituted in recipients will first encounter HTLV-1 Ags, because HTLV-1 still persists in the patients even though proviral loads become undetectable in the peripheral bloods. Indeed, we found that donor-derived Tax155–167-specific CD4$^+$ T cells were present in three ATL patients after allo-HSCT from seronegative donors. This finding also suggests that Tax155–167-specific naive CD4$^+$ T cells may pre-exist in HLA-DRB1*0101$^+$ individuals and can be primed with HTLV-1 Ags during the primary infection. In this study, Tax155–167-specific CD4$^+$ T cells were also detected in an AC and a HAM/TSP patient (Fig. 6B), suggesting that Tax155–167-specific CD4$^+$ T cells may be maintained in some HLA-DR1$^+$ individuals during the chronic phase of HTLV-1 infection. However, it has been reported that epitope hierarchies may change because of T cell escape mutants (43, 44) and unresponsiveness or deletion of epitope-specific T cells because of prolonged Ag stimulation during chronic infection (45, 46). Further longitudinal studies with a number of samples will be required to confirm that Tax155–167 is a dominant epitope of HTLV-1–specific CD4$^+$ T cells in HLA-DRB1*0101$^+$–infected individuals in the course of HTLV-1 infection.

Among three patients (#241, #350, and #364) showing high T cell responses against recombinant Tax protein, two patients (#350 and #364) were found to carry HLA-DRB1*0101 and have efficient CD4$^+$ Th cell responses against Tax155–167. Intriguingly, it has been reported that HLA-DRB1*0101 is associated with susceptibility to HAM/TSP (47, 48). In addition, CD4$^+$ T cells have been shown to be the dominant cells infiltrating in early active inflammatory spinal cord lesions (28, 29) with spontaneous production of proinflammatory cytokines (30). These observations suggest that HLA-DRB1*0101 might be associated with susceptibility to HAM/TSP via an effect on high CD4$^+$ T cell activation. Further studies are needed to clarify whether HLA-DRB1*0101 is associated with high Tax-specific CD4$^+$ T cell responses in HTLV-1–infected individuals.

Early studies using lymphocytic choriomeningitis virus showed that CD4$^+$ T cell help is critical for maintenance of CD8$^+$ T cell function during chronic infections (18). It has also been suggested that CD4$^+$ T cells are required for optimal CTL responses during HTLV-1 infection (49). Aubert et al. (50) showed that both Ag-specific naive and effector CD4$^+$ T cell help rescued exhausted CD8$^+$ T cells in vivo, resulting in a decrease in viral burden. In the current study, we determined a novel HLA-DRB1*0101–restricted Th epitope, Tax155–167, which was capable of augmenting Tax-specific CD8$^+$ T cell expansion by stimulating Tax155–167-specific CD4$^+$ T cells. This epitope would be a useful tool for investigating the roles of HTLV-1–specific CD4$^+$ T cells in antitumor immunity and in pathogenesis of HTLV-1–related inflammatory diseases such as HAM/TSP and developing novel vaccines to prevent progression or recurrence of ATL.

Disclosures

References

1. Hinuma, Y., K. Nagata, M. Hanaoka, M. Nakai, T. Matsumoto, K. I. Kinoshita, S. Shirakawa, and I. Miyoshi. 1981. Adult T-cell leukemia: antigen in an ATL cell line and detection of antibodies to the antigen in human sera. Proc. Natl. Acad. Sci. USA 78: 6476–6480.
2. Poiesz, B. J., F. W. Ruscetti, A. F. Gazdar, P. A. Bunn, J. D. Minna, and R. C. Gallo. 1980. Detection and isolation of type C retrovirus particles from fresh and cultured lymphocytes of a patient with cutaneous T-cell lymphoma. Proc. Natl. Acad. Sci. USA 77: 7415–7419.

3. de Thé, G., and R. Bomford. 1993. An HTLV-I vaccine: why, how, for whom? *AIDS Res. Hum. Retroviruses* 9: 381–386.

4. Uchiyama, T. 1997. Human T cell leukemia virus type I (HTLV-I) and human diseases. *Annu. Rev. Immunol.* 15: 15–37.

5. Tsukasaki, K., T. Maeda, K. Arimura, J. Taguchi, T. Fukushima, Y. Miyazaki, Y. Moriuchi, K. Kuriyama, Y. Yamada, and M. Tomonaga. 1999. Poor outcome of autologous stem cell transplantation for adult T cell leukemia/lymphoma: a case report and review of the literature. *Bone Marrow Transplant.* 23: 87–89.

6. Utsunomiya, A., Y. Miyazaki, Y. Takatsuka, S. Hanada, K. Uozumi, S. Yashiki, M. Tara, F. Kawano, Y. Saburi, H. Kikuchi, et al. 2001. Improved outcome of adult T cell leukemia/lymphoma with allogeneic hematopoietic stem cell transplantation. *Bone Marrow Transplant.* 27: 15–20.

7. Tanosaki, R., N. Uike, A. Utsunomiya, Y. Saburi, M. Masuda, M. Tomonaga, T. Eto, M. Hidaka, M. Harada, I. Choi, et al. 2008. Allogeneic hematopoietic stem cell transplantation using reduced-intensity conditioning for adult T cell leukemia/lymphoma: impact of antithymocyte globulin on clinical outcome. *Biol. Blood Marrow Transplant.* 14: 702–708.

8. Choi, I., R. Tanosaki, N. Uike, A. Utsunomiya, M. Tomonaga, M. Harada, T. Yamanaka, M. Kannagi, and J. Okamura. 2011. Long-term outcomes after hematopoietic SCT for adult T-cell leukemia/lymphoma: results of prospective trials. *Bone Marrow Transplant.* 46: 116–118.

9. Okamura, J., A. Utsunomiya, R. Tanosaki, N. Uike, S. Sonoda, M. Kannagi, M. Tomonaga, M. Harada, N. Kimura, M. Masuda, et al. 2005. Allogeneic stem-cell transplantation with reduced conditioning intensity as a novel immuno-therapy and antiviral therapy for adult T-cell leukemia/lymphoma. *Blood* 105: 4143–4145.

10. Harashima, N., K. Kurihara, A. Utsunomiya, R. Tanosaki, S. Hanabuchi, M. Masuda, T. Ohashi, F. Fukui, A. Hasegawa, T. Masuda, et al. 2004. Graft-versus-Tax response in adult T-cell leukemia patients after hematopoietic stem cell transplantation. *Cancer Res.* 64: 391–399.

11. Jacobson, S., H. Shida, D. E. McFarlin, A. S. Fauci, and S. Koenig. 1990. Circulating CD8+ cytotoxic T lymphocytes specific for HTLV-I pX in patients with HTLV-I associated neurological disease. *Nature* 348: 245–248.

12. Kannagi, M., S. Harada, I. Maruyama, H. Inoko, H. Igarashi, G. Kuwashima, S. Sato, M. Morita, M. Kidokoro, M. Sugimoto, et al. 1991. Predominant recognition of human T cell leukemia virus type I (HTLV-I) pX gene products by human CD8+ cytotoxic T cells directed against HTLV-I-infected cells. *Int. Immunol.* 3: 761–767.

13. Shimizu, Y., A. Takamori, A. Utsunomiya, M. Kurimura, Y. Yamano, M. Hishizawa, A. Hasegawa, F. Kondo, K. Kurihara, N. Harashima, et al. 2009. Impaired Tax-specific T-cell responses with insufficient control of HTLV-1 in a subgroup of individuals at asymptomatic and smoldering stages. *Cancer Sci.* 100: 481–489.

14. Takamori, A., A. Hasegawa, A. Utsunomiya, Y. Maeda, Y. Yamano, M. Masuda, Y. Shimizu, Y. Tamai, A. Sasada, N. Zeng, et al. 2011. Functional impairment of Tax-specific but not cytomegalovirus-specific CD8+ T lymphocytes in a minor population of asymptomatic human T-cell leukemia virus type 1-carriers. *Retrovirology* 8: 100.

15. Cardin, R. D., J. W. Brooks, S. R. Sarawar, and P. C. Doherty. 1996. Progressive loss of CD8+ T cell-mediated control of a gamma-herpesvirus in the absence of CD4+ T cells. *J. Exp. Med.* 184: 863–871.

16. Grakoui, A., N. H. Shoukry, D. J. Woollard, J. H. Han, H. L. Hanson, J. Ghrayeb, K. K. Murthy, C. M. Rice, and C. M. Walker. 2003. HCV persistence and immune evasion in the absence of memory T cell help. *Science* 302: 659–662.

17. Kalams, S. A., S. P. Buchbinder, E. S. Rosenberg, J. M. Billingsley, D. S. Colbert, N. G. Jones, A. K. Shea, A. K. Trocha, and B. D. Walker. 1999. Association between virus-specific cytotoxic T-lymphocyte and helper responses in human immunodeficiency virus type 1 infection. *J. Virol.* 73: 6715–6720.

18. Matloubian, M., R. J. Concepcion, and R. Ahmed. 1994. CD4+ T cells are required to sustain CD8+ cytotoxic T-cell responses during chronic viral infection. *J. Virol.* 68: 8056–8063.

19. Smyk-Pearson, S., I. A. Tester, J. Klarquist, B. E. Palmer, J. M. Pawlotsky, L. Golden-Mason, and H. R. Rosen. 2008. Spontaneous recovery in acute human hepatitis C virus infection: functional T-cell thresholds and relative importance of CD4 help. *J. Virol.* 82: 1827–1837.

20. Jacobson, S., J. S. Reuben, R. D. Streilein, and T. J. Palker. 1991. Induction of CD4+, human T lymphotropic virus type-1-specific cytotoxic T lymphocytes from patients with HAM/TSP: recognition of an immunogenic region of the gp46 envelope glycoprotein of human T lymphotropic virus type-1. *J. Immunol.* 146: 1155–1162.

21. Kitze, B., K. Usuku, Y. Yamano, S. Yashiki, M. Nakamura, T. Fujiyoshi, S. Izumo, M. Osame, and S. Sonoda. 1998. Human CD4+ T lymphocytes recognize a highly conserved epitope of human T lymphotropic virus type 1 (HTLV-1) env gp21 restricted by HLA DRB1*0101. *Clin. Exp. Immunol.* 111: 278–285.

22. Kobayashi, H., T. Ngato, K. Sato, N. Aoki, S. Kimura, Y. Tanaka, H. Aizawa, M. Tateno, and E. Celis. 2006. In vitro peptide immunization of target tax protein human T-cell leukemia virus type 1-specific CD4+ helper T lymphocytes. *Clin. Cancer Res.* 12: 3814–3822.

23. Yamano, Y., B. Kitze, S. Yashiki, K. Usuku, T. Fujiyoshi, T. Kaminagayoshi, K. Unoki, S. Izumo, M. Osame, and S. Sonoda. 1997. Preferential recognition of synthetic peptides from HTLV-I gp21 envelope protein by HLA-DRB1 alleles associated with HAM/TSP (HTLV-I-associated myelopathy/tropical spastic paraparesis). *J. Neuroimmunol.* 76: 50–60.

24. Goon, P. K., T. Igakura, E. Hanon, A. J. Mosley, A. Barfield, A. L. Barnard, L. Kaftantzi, Y. Tanaka, G. P. Taylor, J. N. Weber, and C. R. Bangham. 2004. Human T cell lymphotropic virus type I (HTLV-I)-specific CD4+ T cells:

25. Toulza, F., A. Heaps, Y. Tanaka, G. P. Taylor, and C. R. Bangham. 2008. High frequency of CD4+FoxP3+ cells in HTLV-1 infection: inverse correlation with HTLV-1-specific CTL response. *Blood* 111: 5047–5053.

26. Satou, Y., J. Yasunaga, M. Yoshida, and M. Matsuoka. 2006. HTLV-I basic leucine zipper factor gene mRNA supports proliferation of adult T cell leukemia cells. *Proc. Natl. Acad. Sci. USA* 103: 720–725.

27. Sugata, K., Y. Satou, J. Yasunaga, H. Hara, K. Ohshima, A. Utsunomiya, M. Mitsuyama, and M. Matsuoka. 2012. HTLV-1 bZIP factor impairs cell-mediated immunity by suppressing production of Th1 cytokines. *Blood* 119: 434–444.

28. Iwasaki, Y., Y. Ohara, I. Kobayashi, and S. Akizuki. 1992. Infiltration of helper/inducer T lymphocytes heralds central nervous system damage in human T-cell leukemia virus infection. *Am. J. Pathol.* 140: 1003–1008.

29. Umehara, F., S. Izumo, M. Nakagawa, A. T. Ronquillo, K. Takahashi, K. Matsumuro, E. Sato, and M. Osame. 1993. Immunocytochemical analysis of the cellular infiltrate in the spinal cord lesions in HTLV-I-associated myelopathy. *J. Neuropathol. Exp. Neurol.* 52: 424–430.

30. Umehara, F., S. Izumo, A. T. Ronquillo, K. Matsumuro, E. Sato, and M. Osame. 1994. Cytokine expression in the spinal cord lesions in HTLV-I-associated myelopathy. *J. Neuropathol. Exp. Neurol.* 53: 72–77.

31. Kurihara, K., Y. Shimizu, A. Takamori, N. Harashima, M. Noji, T. Masuda, A. Utsunomiya, J. Okamura, and M. Kannagi. 2006. Human T-cell leukemia virus type-I (HTLV-I)-specific T-cell responses detected using three-divided glutathione-S-transferase (GST)-Tax fusion proteins. *J. Immunol. Methods* 313: 61–73.

32. Harashima, N., R. Tanosaki, Y. Shimizu, K. Kurihara, T. Masuda, J. Okamura, and M. Kannagi. 2005. Identification of two new HLA-A*1101-restricted tax epitopes recognized by cytotoxic T lymphocytes in an adult T-cell leukemia patient after hematopoietic stem cell transplantation. *J. Virol.* 79: 10088–10092.

33. Rammensee, H. G., T. Friede, and S. Stevanoviíc. 1995. MHC ligands and peptide motifs: first listing. *Immunogenetics* 41: 178–228.

34. Hanon, E., S. Hall, G. P. Taylor, M. Saito, R. Davis, Y. Tanaka, K. Usuku, M. Osame, J. N. Weber, and C. R. Bangham. 2000. Abundant tax protein expression in CD4+ T cells infected with human T-cell lymphotropic virus type I (HTLV-I) is prevented by cytotoxic T lymphocytes. *Blood* 95: 1386–1392.

35. Richardson, J. H., A. J. Edwards, J. K. Cruickshank, P. Rudge, and A. G. Dalgleish. 1990. In vivo cellular tropism of human T-cell leukemia virus type 1. *J. Virol.* 64: 5682–5687.

36. Sakai, J. A., M. Nagai, M. B. Brennan, C. A. Mora, and S. Jacobson. 2001. In vitro spontaneous lymphoproliferation in patients with human T-cell lymphotropic virus type I-associated neurologic disease: predominant expansion of CD8+ T cells. *Blood* 98: 1506–1511.

37. Elovaara, I., S. Koenig, A. Y. Brewah, R. M. Woods, T. Lehky, and S. Jacobson. 1993. High human T cell lymphotropic virus type 1 (HTLV-1)-specific precursor cytotoxic T lymphocyte frequencies in patients with HTLV-1-associated neurological disease. *J. Exp. Med.* 177: 1567–1573.

38. Kannagi, M., H. Shida, H. Igarashi, K. Kuruma, H. Murai, Y. Aono, I. Maruyama, M. Osame, T. Hattori, H. Inoko, et al. 1992. Target epitope in the Tax protein of human T-cell leukemia virus type I recognized by class I major histocompatibility complex-restricted cytotoxic T cells. *J. Virol.* 66: 2928–2933.

39. Pique, C., A. Ureta-Vidal, A. Gessain, B. Chancerel, O. Gout, R. Tamouza, F. Agis, and M. C. Dokhélar. 2000. Evidence for the chronic in vivo production of human T cell leukemia virus type I Rof and Tof proteins from cytotoxic T lymphocytes directed against viral peptides. *J. Exp. Med.* 191: 567–572.

40. Sundaram, R., Y. Sun, C. M. Walker, F. A. Lemonnier, S. Jacobson, and P. T. Kaumaya. 2003. A novel multivalent human CTL peptide construct elicits robust cellular immune responses in HLA-A*0201 transgenic mice: implications for HTLV-1 vaccine design. *Vaccine* 21: 2767–2781.

41. Vollers, S. S., and L. J. Stern. 2008. Class II major histocompatibility complex tetramer staining: progress, problems, and prospects. *Immunology* 123: 305–313.

42. Sabatino, J. J., Jr., J. Huang, C. Zhu, and B. D. Evavold. 2011. High prevalence of low affinity peptide-MHC II tetramer-negative effectors during polyclonal CD4+ T cell responses. *J. Exp. Med.* 208: 81–90.

43. Goulder, P. J., A. K. Sewell, D. G. Lalloo, D. A. Price, J. A. Whelan, J. Evans, G. P. Taylor, G. Luzzi, P. Giangrande, R. E. Phillips, and A. J. McMichael. 1997. Patterns of immunodominance in HIV-1-specific cytotoxic T lymphocyte responses in two human histocompatibility leukocyte antigens (HLA)-identical siblings with HLA-A*0201 are influenced by epitope mutation. *J. Exp. Med.* 185: 1423–1433.

44. Nowak, M. A., R. M. May, R. E. Phillips, S. Rowland-Jones, D. G. Lalloo, S. McAdam, P. Klenerman, B. Köppe, K. Sigmund, C. R. Bangham, et al. 1995. Antigenic oscillations and shifting immunodominance in HIV-1 infections. *Nature* 375: 606–611.

45. Goulder, P. J., M. A. Altfeld, E. S. Rosenberg, T. Nguyen, Y. Tang, R. L. Eldridge, M. M. Addo, S. He, J. S. Mukherjee, M. N. Phillips, et al. 2001. Substantial differences in specificity of HIV-specific cytotoxic T cells in acute and chronic HIV infection. *J. Exp. Med.* 193: 181–194.

46. Wherry, E. J., J. N. Blattman, K. Murali-Krishna, R. van der Most, and R. Ahmed. 2003. Viral persistence alters CD8 T-cell immunodominance and tissue distribution and results in distinct stages of functional impairment. *J. Virol.* 77: 4911–4927.

47. Jeffery, K. J., K. Usuku, S. E. Hall, W. Matsumoto, G. P. Taylor, J. Procter, M. Bunce, G. S. Ogg, K. I. Welsh, J. N. Weber, et al. 1999. HLA alleles de-

termine human T-lymphotropic virus-I (HTLV-I) proviral load and the risk of HTLV-I-associated myelopathy. *Proc. Natl. Acad. Sci. USA* 96: 3848–3853.

48. Sabouri, A. H., M. Saito, K. Usuku, S. N. Bajestan, M. Mahmoudi, M. Forughipour, Z. Sabouri, Z. Abbaspour, M. E. Goharjoo, E. Khayami, et al. 2005. Differences in viral and host genetic risk factors for development of human T-cell lymphotropic virus type 1 (HTLV-1)-associated myelopathy/tropical spastic paraparesis between Iranian and Japanese HTLV-1-infected individuals. *J. Gen. Virol.* 86: 773–781.

49. Kurihara, K., N. Harashima, S. Hanabuchi, M. Masuda, A. Utsunomiya, R. Tanosaki, M. Tomonaga, T. Ohashi, A. Hasegawa, T. Masuda, et al. 2005. Potential immunogenicity of adult T cell leukemia cells in vivo. *Int. J. Cancer* 114: 257–267.

50. Aubert, R. D., A. O. Kamphorst, S. Sarkar, V. Vezys, S. J. Ha, D. L. Barber, L. Ye, A. H. Sharpe, G. J. Freeman, and R. Ahmed. 2011. Antigen-specific CD4 T-cell help rescues exhausted CD8 T cells during chronic viral infection. *Proc. Natl. Acad. Sci. USA* 108: 21182–21187.

blood

Preapoptotic protease calpain-2 is frequently suppressed in adult T-cell leukemia

Makoto Ishihara, Natsumi Araya, Tomoo Sato, Ayako Tatsuguchi, Naomi Saichi, Atae Utsunomiya, Yusuke Nakamura, Hidewaki Nakagawa, Yoshihisa Yamano and Koji Ueda

---

Updated information and services can be found at:
http://bloodjournal.hematologylibrary.org/content/121/21/4340.full.html

Articles on similar topics can be found in the following Blood collections
    Lymphoid Neoplasia (1404 articles)

Information about reproducing this article in parts or in its entirety may be found online at:
http://bloodjournal.hematologylibrary.org/site/misc/rights.xhtml#repub_requests

Information about ordering reprints may be found online at:
http://bloodjournal.hematologylibrary.org/site/misc/rights.xhtml#reprints

Information about subscriptions and ASH membership may be found online at:
http://bloodjournal.hematologylibrary.org/site/subscriptions/index.xhtml

LYMPHOID NEOPLASIA

Preapoptotic protease calpain-2 is frequently suppressed in adult T-cell leukemia

Makoto Ishihara,[1] Natsumi Araya,[2] Tomoo Sato,[2] Ayako Tatsuguchi,[1] Naomi Saichi,[1] Atae Utsunomiya,[3] Yusuke Nakamura,[4] Hidewaki Nakagawa,[1] Yoshihisa Yamano,[2] and Koji Ueda[1]

[1]Laboratory for Biomarker Development, Center of Genomic Medicine, RIKEN, Tokyo, Japan; [2]Department of Molecular Medical Science, Institute of Medical Science, St. Marianna University School of Medicine, Kawasaki, Japan; [3]Department of Hematology, Imamura Bun-in Hospital, Kagoshima, Japan; and [4]Section of Hematology/Oncology, Department of Medicine Faculty, The University of Chicago, Chicago, IL

Key Points

● Proteome-wide analysis of HTLV-1–infected T cells identified 17 biomarker proteins for the diagnosis of ATL or HAM/TSP patients.

Adult T-cell leukemia (ATL) is one of the most aggressive hematologic malignancies caused by human T-lymphotropic virus type 1 (HTLV-1) infection. The prognosis of ATL is extremely poor; however, effective strategies for diagnosis and treatment have not been established. To identify novel therapeutic targets and diagnostic markers for ATL, we employed focused proteomic profiling of the $CD4^+CD25^+CCR4^+$ T-cell subpopulation in which HTLV-1–infected cells were enriched. Comprehensive quantification of 14 064 peptides and subsequent 2-step statistical analysis using 29 cases (6 uninfected controls, 5 asymptomatic carriers, 9 HTLV-1–associated myelopathy/tropical spastic paraparesis patients, 9 ATL patients) identified 91 peptide determinants that statistically classified 4 clinical groups with an accuracy rate of 92.2% by cross-validation test. Among the identified 17 classifier proteins, α-II spectrin was drastically accumulated in infected T cells derived from ATL patients, whereas its digestive protease calpain-2 (CAN2) was significantly downregulated. Further cell cycle analysis and cell growth assay revealed that rescue of CAN2 activity by overexpressing constitutively active CAN2 (Δ_{19}CAN2) could induce remarkable cell death on ATL cells accompanied by reduction of α-II spectrin. These results support that proteomic profiling of HTLV-1–infected T cells could provide potential diagnostic biomarkers and an attractive resource of therapeutic targets for ATL. (*Blood*. 2013;121(21):4340-4347)

Introduction

Human T-lymphotropic virus type 1 (HTLV-1) is a human retrovirus that is the pathogenic agent of HTLV-1–associated diseases, such as adult T-cell leukemia (ATL) and HTLV-1–associated myelopathy/tropical spastic paraparesis (HAM/TSP). Recent epidemiological studies revealed that HTLV-1 is endemic mainly in Japan, the Caribbean basin, Iran, Africa, South America, and the Melanesian islands.[1] Other estimates have shown that 20 million to 30 million people worldwide are infected with HTLV-1.[2] The infection is followed by a prolonged asymptomatic phase of 20 to 30 years, and 2% to 5% of the infected individuals develop ATL during their lifetime.[3] ATL is one of the most aggressive hematologic malignancies characterized by increased numbers of lymphocytes with multilobulated nuclei, so-called flower cells, in blood circulation. The prognosis is severe with the median overall survival period and 5-year survival rate of ATL patients of 7 months and 20%, respectively.[4] Recently, humanized anti-CCR4 (KW-0761) therapeutic antibody achieved a great improvement in ATL treatment in a phase 3 study. However, the disease control rate was restricted to 50%, and long-term prognosis has yet to be known.[5] For future improvements in the management of ATL, novel biomarkers for early diagnosis are urgently needed for early therapeutic intervention.

To date, comprehensive genomic or proteomic studies using $CD4^+$ T cells have been performed for this purpose,[6-9] but reproducibility and reliability of quantification results in the discovery phase were uncertain due to the diverse individual variety of HTLV-1–infected cell contents in $CD4^+$ T cells. To overcome the etiologic variety of samples, we focused on the $CD4^+CD25^+CCR4^+$ T-cell subpopulation since Yamano et al[10] recently revealed that HTLV-1 preferentially infected $CD4^+CD25^+CCR4^+$ T cells in both ATL and HAM/TSP patients. By targeting $CD4^+CD25^+CCR4^+$ T cells, we here provide the first quantitative proteome map illustrating molecular disorders in pathogenic human T cells directly associated with the onset or progression of ATL. The comprehensive and comparative interpretation of total proteome in infected cells, especially between asymptomatic HTLV-1 carriers and ATL patients, could immediately lead to specific candidates for biomarkers and drugs.

Another challenge to emphasize in this study is our recently established proteomic profiling technologies. It is indisputable that the greater the number of clinical samples analyzed, the more confidently statistical analysis can be undertaken in order to identify diagnostic markers and druggable targets. Despite this fact, previous proteomics reports could not provide high-throughput quantitative methodologies that were sufficient for dealing with even more than 10 clinical samples, excepting a study utilizing a surface enhanced laser desorption/ionization time of flight mass spectrometer. Although the surface enhanced laser desorption/ionization time of flight method drastically improved the performance in both quantification and throughput, allowing relative quantification

analysis for 96 samples in several hours, at most only 250 unidentified protein peaks were detectable. In the present study, we integrated the proteomics server for the huge data set "Expressionist" (Genedata A.G., Basel, Switzerland) with high-end mass spectrometers to maximize the quality and quantity of protein catalogs transferred from mass spectrometers. We first describe the discovery phase providing a panel of novel diagnostic molecules from quantification of 14 064 peptides and identification of 4763 proteins. As the functional validation phase, we further examined the physiological potential of an identified diagnostic marker candidate, calpain-2 (CAN2), particularly concerning the association of its activity with survival or progression of ATL cells.

Materials and methods

PBMCs and cell lines

Peripheral blood mononuclear cells (PBMCs) from 6 normal donors, 5 asymptomatic carriers, and 9 HAM/TSP patients used in the screening analysis were collected in the St. Marianna University School of Medicine. Those from 9 ATL patients were collected in the Imamura Bun-in Hospital. PBMCs from 4 ATL patients used for the validation experiments were provided by the Joint Study on Predisposing Factors of ATL Development. The others from 4 HAM/TSP patients were collected in the St. Marianna University School of Medicine. The use of these human specimens in this study was approved by individual institutional ethical committees: the Ethical Committee of Yokohama Institute, RIKEN (approval code Yokohama H22-3); the Ethical Committee of St. Marianna University School of Medicine; the Institutional Review Board of Imamura Bun-in Hospital; and the Ethical Committee of the University of Tokyo (approval code 10-50). This study was conducted in accordance with the Declaration of Helsinki.

SO-4, KOB, and KK1 cells were kindly provided by Dr Yasuaki Yamada, cultured in RPMI 1640 supplemented with 10% fetal bovine serum (Cell Culture Bioscience, Tokyo, Japan), 100 kU/L interleukin 2 (Cell Science & Technology Institute Inc., Tokyo, Japan), and 1 × antibiotic-antimycotic solution (Sigma-Aldrich, MO). Jurkat, SUP-T1, CCRF-CEM, and MOLT-3 cells were cultured in RPMI 1640 supplemented with 10% fetal bovine serum and 1 × antibiotic-antimycotic solution. All cell lines were grown at 37°C in 5% CO_2. $CD3^+CD4^+CD25^+CCR4^+$ T cells were isolated with anti-CD3-FITC (eBioscience, San Diego, CA), anti-CCR4-PE (Becton Dickinson, CA), anti-CD4-Cy7 (eBioscience), and anti-CD25-APC (eBioscience) on a Cell Sorter JSAN (Bay Bioscience, Hyogo, Japan).

Sample preparation for mass spectrometric analysis

The $CD4^+CD25^+CCR4^+$ T cells were washed with phosphate-buffered saline 3 times and lysed in denaturation buffer (8 M urea in 50 mM ammonium bicarbonate). After sonication, reduction with 5 mM tris(2-carboxyethyl) phosphine (Sigma-Aldrich) at 37°C for 30 minutes, and alkylation with 25 mM iodacetamide (Sigma-Aldrich) at room temperature for 45 minutes, lysates were digested with Trypsin GOLD (Promega, WI) with protein/enzyme ratio of 25:1 at 37°C for 12 hours. The digested peptides were desalted with Oasis HLB μElution plate (Waters, MA). The collected samples were dried up with a Vacuum Spin Drier (TAITEC Co. Ltd., Saitama, Japan) and subjected to mass spectrometric analyses.

Liquid chromatography tandem mass spectrometry (LC/MS/MS)

The digested peptides were separated on a 0.1 × 200 mm homemade C_{18} column using a 2-step linear gradient, 2% to 35% acetonitrile for 95 minutes and 35% to 95% acetonitrile for 15 minutes in 0.1% formic acid with a flow rate of 200 nL/min. The eluting peptides were analyzed with a QSTAR-Elite mass spectrometer (AB Sciex, CA) in the smart information-dependent acquisition mode of Analyst QS software 2.0 (AB Sciex). The other parameters on QSTAR-Elite were shown as follows: DP = 60, FP = 265, DP2 = 15, CAD = 5, IRD = 6, IRW = 5, curtain gas = 20, and ion spray voltage = 2000 V.

Two-dimensional (2D) LC/MS/MS

Tryptic digests of $CD4^+CD25^+CCR4^+$ T cells were dissolved in 10 mM ammonium formate in 25% acetonitrile and fractionated by a 0.2 × 250 mm monolith strong cation exchange column (GL Science, Tokyo, Japan). Peptides were eluted with an ammonium formate gradient from 10 mM to 1 M in curve = 3 mode for 70 minutes using a Prominence high-performance liquid chromatography (HPLC) system (Shimadzu Corporation, Kyoto, Japan). The eluate was fractionated into 20 fractions and analyzed individually by LTQ-Orbitrap-Velos mass spectrometer (Thermo Scientific, Bremen, Germany) accompanied with the Ultimate 3000 nano-HPLC system. The fractionated peptide samples were separated with the same gradient used in the QSTAR-Elite system described previously and analyzed by LTQ-Orbitrap-Velos acquiring a full MS scan on Fourier-transition mode with MS resolution = 60 000 and simultaneously MS/MS scans for the 20 most intense precursor ions in each MS spectrum on ion-trap mode with regular resolution. Other important parameters for LTQ-Orbitrap-Velos were as follows: capillary temp = 250, source voltage = 2 kV, MS scan range = mass-to-charge ratio (m/z) 400 to 1600, acquire data dependent CID MS/MS for top-20 intense precursors, and dynamic exclusion enabled during 30 seconds. For protein identification, all MS/MS spectra were searched against SwissProt database version 2012_06 (20 232 human protein sequences) using SEQUEST algorithm on ProteomeDiscoverer 1.3 software (Thermo Scientific) with the following parameters: MS tolerance = 3 ppm, MS/MS tolerance = 0.8 Da, maximum missed cleavages = 2, enzyme = trypsin, taxonomy = Homo sapiens, fixed modification = carbamidomethylation on cysteine, and variable modification = oxidation on methionine. We accepted the protein identification satisfying the false discovery rate <1% by Percolator false discovery rate estimation algorithm on ProteomeDiscoverer.

Label-free quantification analysis

The LC/MS/MS raw data were imported into the Expressionist RefinerMS module and subjected to the following data processing and relative quantification steps. The total work flow on the RefinerMS module is shown in supplemental Figure 1 (see the Blood Web site). The LC/MS/MS raw data set from 29 clinical samples was displayed in 2D planes (m/z vs retention time [RT]). The chromatogram grid was applied to all planes: scan counts = 10, polynom order = 3, and RT smoothing = 0. The planes were simplified by subtracting background noises using chromatogram chemical noise subtraction: RT window = 50 scans, quantile subtraction = 50%, and RT smoothing = 3 scans. After the noise subtraction, data points with intensity <10 were clipped to zero. The RT variety among 29 planes was adjusted by chromatogram RT alignment: RT transformation window = 0.2 minutes, RT search interval = 5 minutes, m/z window = 0.1 Da, and gap penalty = 1. Peaks were detected by chromatogram summed peak detection: summation window = 5 scans, overlap = 50, minimum peak size = 4 scans, maximum merge distance = 10 points, peak RT splitting = true, intensity profiling = max, gap/peak ratio = 1%, refinement threshold = 5, consistency threshold = 0.8, and signal/noise threshold = 1. The detected peaks were grouped into isotopic clusters derived from each molecule using 2-step chromatogram isotopic peak clustering. The first parameters were as follows: minimum charge = 1, maximum charge = 10, maximum missing peaks = 0, first allowed gap position = 3, RT window = 0.1 minute, m/z tolerance = 0.05 Da, isotope shape tolerance = 10, and minimum cluster size ration = 1.2. The second parameters were as follows: minimum charge = 1, maximum charge = 10, maximum missing peaks = 0, first allowed gap position = 3, RT window = 0.1 minute, m/z tolerance = 0.05 Da, and minimum cluster size ration = 0.6.

Expression vectors and siRNA

For the $\Delta_{19}CAN2$ construct, the CAPN2 fragment was amplified with primers 5'-CATGTCGACTCCCACGAGAGGGCCATCAAGT-3' and 5'-CATTC-TAGATCAAAGTACTGAGAAACAGAGCC-3' from pBlueBacIII CAPN2 and cloned into pEFBOS-Myc. Prior to the overexpression experiments, we confirmed that the sequence of the inserted CAPN2 fragment was identical to the Mammalian Gene Collection sequence (accession number
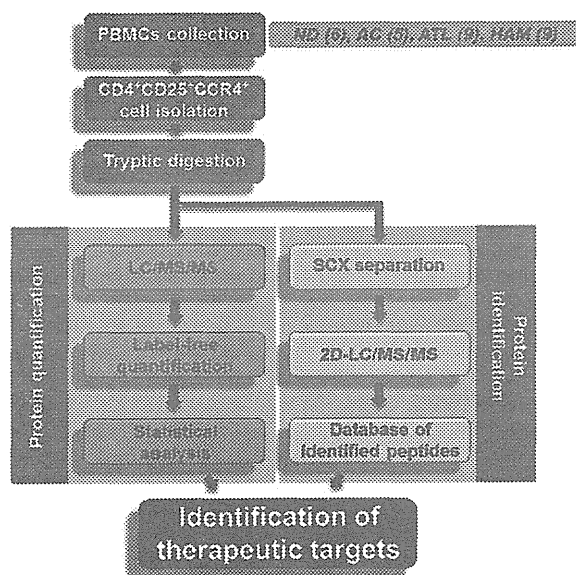
Figure 1. Schematic overview of proteomic profiling for CD4$^+$CD25$^+$CCR4$^+$ cells. PBMCs were collected from 6 normal donors, 5 asymptomatic carriers, 9 ATL patients, and 9 HAM/TSP patients, followed by isolation of the CD4$^+$CD25$^+$CCR4$^+$ subset using the cell-sorting system. The statistical candidate selection steps, including LC/MS/MS data processing, label-free quantification, and statistical analysis, were performed on the Expressionist proteome server. The protein identification database was separately established based on 2D LC/MS/MS analysis. ND, normal donors; AC, asymptomatic carriers.

BC021303). The 5-μg vector DNA was transfected to 1×10^6 cells. The small interfering RNAs (siRNAs) against SPTAN1, PTMS, HSPE1, and SHMT2 and siRNA universal negative control were purchased from Sigma-Aldrich. The 500-pmol siRNA oligo was transfected into 1×10^6 cells. The vectors and siRNAs were transfected into all cell lines except CCRF-CEM by Amaxa Nucleoportator transfection Kit V (Lonza, Cologne, Germany) and CCRF-CEM by Kit C (Lonza).

Cell cycle analysis and proliferation assay

For the cell cycle analysis, 1×10^5 to 2×10^5 cells were washed and agitated in 0.1% Triton-X (Sigma-Aldrich) with 100 ng/mL of ribonuclease (Sigma-Aldrich). Following addition of 1 μg/mL propidium iodide, the flow cytometric analysis was performed on FACScalibur (Becton Dickinson). The data analysis was performed using FlowJo software (Tree Star Inc., OR). Doublet events were eliminated from analyses by proper gating on FL2-W/FL2-A primary plots before histogram analysis of DNA content. Cell proliferation was estimated by measuring cell metabolic activity using Cell Counting Kit-8 (Dojindo, Kumamoto, Japan) following the manufacturer's recommendation.

Western blotting

Cells were lysed in lysis buffer [1% NP-40, 2 mM EGTA, 2 mM MgCl$_2$, 150 mM NaCl, 20 mM tris(hydroxymethyl)aminomethane–HCl (pH 7.5), 10% glycerol, containing the protease inhibitor cocktail Complete (Roche, IN)] and subjected to sodium dodecyl sulfate–polyacrylamide gel electrophoresis and transferred onto PVDF membranes. Following blocking with 4% Block Ace (Yukijirushi Nyugyo Inc., Tokyo, Japan), membranes were incubated with anti-myc (9E10; Sigma-Aldrich) or anti-α-II spectrin (Abcam, Cambridge, UK) antibodies. Membranes were then incubated with horseradish peroxidase–conjugated anti-mouse IgG (GE Healthcare, NJ) or anti-rabbit IgG (GE Healthcare), respectively, and visualized with Western Lightning kit (Perkin Elmer, MA).

Multiple reaction monitoring (MRM)

CD4$^+$ T cells were isolated from PBMCs using flow cytometry. The tryptic digests of the isolated cells were analyzed by 4000 Q-TRAP mass

spectrometer (AB Sciex) accompanied with Ultimate 3000 nano-HPLC system. The LC gradient was as follows: 2% to 30% acetonitrile for 10 minutes and 30% to 95% acetonitrile for 5 minutes in 0.1% formic acid with a flow rate of 300 nL/min. The MRM transitions monitored were m/z 409.7/375.2 for α-II spectrin (SPTA2); m/z 538.3/889.5 for parathymosin (PTMS); m/z 507.3/147.1 for heat shock 10-kDa protein, mitochondrial (CH10); m/z 490.3/147.1 for serine hydroxymethyltransferase, mitochondrial (GLYM); and m/z 581.3/919.5 for β-actin, respectively. Individual peak areas were normalized by the peak area of β-actin. Data acquisition was performed with ion spray voltage = 2300 V, curtain gas = 10 psi, nebulizer gas = 10 psi, and an interface heating temperature = 150°C. The parameters were set as follows: declustering potential = 60, entrance potential = 10, collision cell exit potential = 10, and dwell time for each transition = 10 seconds. Collision energy was optimized to achieve maximum intensity for each MRM transition as follows: 34.03 V for m/z 409.7/175.1, 24.68 eV for m/z 538.3/889.5, 23.32 eV for m/z 507.3/147.1, 37.57 eV for m/z 490.3/147.1, and 31.58 eV for m/z 581.3/919.5.

Results

Quantitative proteome profiling of CD4$^+$CD25$^+$CCR4$^+$ T cells

A schematic overview of the screening approach is shown in Figure 1. To identify diagnostic markers expressed in HTLV-1–infected T cells, a CD4$^+$CD25$^+$CCR4$^+$ subset of PBMCs from 6 uninfected volunteers, 5 asymptomatic carriers, 9 HAM/TSP patients, and 9 ATL patients was isolated by flow cytometry (Figure 2). The averaged proportion of CD4$^+$CD25$^+$CCR4$^+$ cells in CD4$^+$ T cells from 4 clinical groups was 6.48 ± 2.46%, 13.17 ± 13.06%, 20.55 ± 10.73%, and 55.83 ± 22.40%, respectively, indicating that the occupancy of viral reservoir cells varied drastically among both pathological groups and even individuals within a group. Enrichment of the infected cells was confirmed by viral load measurement of the used samples (supplemental Figure 2). As reported previously,[10] the viral load of CD4$^+$CD25$^+$CCR4$^+$ cells (37.91 copies/100 cells on average) was ~10 times higher than that of CD4$^+$CD25$^-$CCR4$^-$ cells (4.12 copies/100 cells on average), indicating that the former cells were evidently the HTLV-1–enriched fraction. This fact strongly supports the importance of
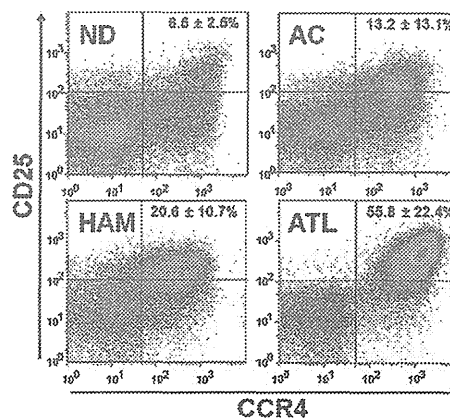

**Figure 2. Representative sorting results of CD4$^+$CD25$^+$CCR4$^+$ cells.** After labeling with anti-CD3-FITC, anti-CD4-Cy7, anti-CD25-APC, and anti-CCR4-PE, the CD3$^+$CD4$^+$CD25$^+$CCR4$^+$ fraction was isolated. The averaged content ± standard deviation (%) of CD25$^+$CCR4$^+$ cells out of CD3$^+$CD4$^+$ cells was calculated for each clinical group and is displayed in the upper right section of the panels.

Figure 3. Statistical extraction of candidate thera-peutic targets. The 14 064 nonredundant peptides detected were subjected to a 4-group Kruskal-Wallis test (ND, AC, ATL, and HAM), resulting in identification of 1170 first candidates ($P < .01$). ND, normal donors; AC, asymptomatic carriers. (A) Next, the Expressionist ranking method further narrowed down the candidates to 91 peptides based on SVM-REF so that the misclassifica-tion rate in the cross-validation test became minimum, 7.8%. (B) The predicted classification result by leave-one-out cross-validation test. The 27 out of 29 cases were successfully classified into the true classes. (C) The three-dimensional plot shows the additional assessment for the classification power of 91 classifiers by principal component analysis. Comp. 1 to 3 indicate principal components 1 to 3.
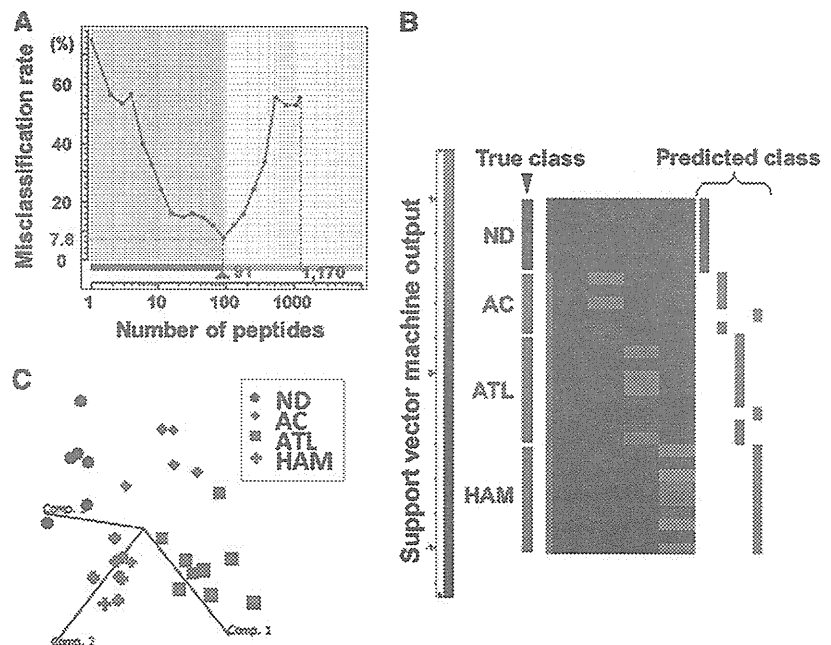
enriching pathogenic cells for rigorous quantitative biomarker discovery.

An accurately adjusted number of CD4⁺CD25⁺CCR4⁺ cells from 29 cases were digested with trypsin and subjected to LC/MS/MS analysis individually. Because recent mass spectrometers often deal with data on the order of hundreds of megabytes per sample, it has been considered almost impossible to calculate a data set larger than a gigabyte from large-scale clinical samples on desktop computers. Hence, we constructed a proteomics server equipped with a 12-core central processing unit, 36 SAS hard disks, and 192-GB physical memories driving the Expressionist, which was designed to combine the database module, the data processing module, and the statistical analysis module into a single integrative platform for genomics, proteomics, and metabolomics. The detailed work flow for data processing and quantification for 29 LC/MS/MS raw data was described in the "Materials and methods" and is illustrated in supplemental Figure 1. Finally, 68 454 nonredundant peaks were detected and grouped into 37 143 isotopic clusters, or molecules. As tryptic peptides should appear as multivalent ions in electrospray ionization mass spectra, 23 079 singly charged ions were removed, resulting in utilization of 14 064 peptide signals for further statistical selection of diagnostic markers.

Statistical identification of candidate diagnostic markers for ATL

A stepwise statistical extraction was employed for the effective identification of proteins, which demonstrated specific up- or downregulation in the ATL group. In the first stage, a 4-group Kruskal-Wallis test was performed to roughly extract the candidates showing a significantly distinct expression level among 4 clinical groups. Here we set the cutoff line at $P < .01$ and obtained 1170 first candidate peptides simply because the isolated peptide set using this criterion showed the best performance in the following prediction model.

Next, we selected the final candidates by the support vector machine–recursive feature elimination algorithm in the Expressionist Analyst module. Support vector machine–recursive feature elimination

is a candidate elimination method based on SVM, which enabled us to improve the classification outputs by selecting the best-performing peptide set among initially provided candidates.[11] As a result, a combination of 91 peptides showed the lowest mis-classification rate (7.78%) in a leave-one-out cross-validation test (Figure 3A-B). To evaluate the classification efficiency of 91 selected candidates, the principal component analysis was performed. Figure 3C shows the three-dimensional plot of 29 clinical samples based on the 3 best-explainable components, which illustrated statistically clear segregation among the 4 clinical groups. These assessments indicated that the 91 peptides should be a sufficient set of classifiers that closely associated with the pathological characteristics of the 4 clinical groups.

Based on an independently constructed 6279-protein identifi-cation database for CD4⁺CD25⁺CCR4⁺ cells using 2D LC/MS/MS (see details in "Materials and methods"), 19 peptides among the 91 candidate peptides were successfully assigned to 17 proteins listed in Table 1. The mass spectrometric quantification profiles for the 19 peptides are also shown in Figure 4 (box plots).

Recovering CAN2 activity induced cell death in ATL cells

Our diagnostic marker discovery for ATL identified an enzyme-substrate pair, CAN2 and SPTA2, which demonstrated significantly aberrant expression level in ATL patients (Figure 4). Interestingly, the intensities of the 2 proteins in 27 screening cases (without 2 statistical outliers in Figure 4) showed a clearly inverse correlation ($R^2 = 0.395$, Figure 5A). To examine whether CAN2 down-regulation and/or SPTA2 upregulation might be essential for the growth of ATL cells, the enzymatic activity of CAN2 was rescued by overexpressing the constitutively active form of CAN2 (Δ_{19}CAN2) in 3 ATL cell lines, SO-4, KOB, and KK1. After 36 hours of transfection, significant inhibition of cell proliferation (Figure 5B) and induction of sub-G1 transition was observed by activation of CAN2 in 3 ATL cells, but not in 4 non-ATL leukemia cell lines (Figure 5C). Furthermore, overexpression of Δ_{19}CAN2 drastically attenuated the expression level of SPTA2 in the ATL cell

Table 1. List of 17 protein classifiers for categorization of normal donors, asymptomatic carriers, HAM/TSP, and ATL

Accession	Protein name	P value (Kruskal-Wallis test)	m/z	RT	Charge	Peptide score	Identity or homology threshold	Sequence
LPPL	Eosinophil lysophospholipase	2.3.E-03	409.722	47.4	2	36.3	27	MVQVWR
CH10	Heat shock 10-kDa protein, mitochondrial	2.5.E-03	430.721	40.6	2	26.2	21	GGIMLPEK
PRG2	Bone marrow proteoglycan	2.4.E-03	528.271	64.6	2	31.6	28	RLPFICSY
MOES	Moesin	8.1.E-04	532.253	26.8	2	46.2	29	EKEELMER
MNDA	Myeloid cell nuclear differentiation antigen	9.4.E-03	647.863	69.1	2	67.3	24	SLLAYDLGLTTK
GLYM	Serine hydroxymethyltransferase, mitochondrial	8.7.E-04	408.551	21.6	3	31.1	18	HADIVTTTTHK
PTMS	Parathymosin	9.7.E-04	453.875	17.8	3	41.2	25	AAEEEDEADPKR
TPIS	Triosephosphate isomerase	9.1.E-03	472.266	71.0	3	54.0	28	QSLGELIGTLNAAK
HSP71	Heat shock 70-kDa protein 1A/1B	9.7.E-03	563.307	65.5	3	93.8	21	IINEPTAAAIAYGLDR
CD6	T-cell differentiation antigen CD6	7.7.E-03	592.306	37.8	3	62.7	22	VLCQSLGCGTAVERPK
ANXA1	Annexin A1	4.4.E-04	612.347	61.5	3	57.0	17	RKGTDVNVFNTILTTR
ANXA6	Annexin A6	2.3.E-03	669.017	70.9	3	54.7	16	AMEGAGTDEKALIEILATR
SPTA2	Spectrin α chain, brain	5.4.E-03	409.718	28.8	2	42.7	30	EAGSVSLR
GLYM	Serine hydroxymethyltransferase, mitochondrial	1.1.E-03	428.240	57.0	2	42.8	27	SGLIFYR
DRB1s	HLA class II histocompatibility antigen, DRB1-1, 4, 10, 11, 13, 15, 16 β chain	1.0.E-02	478.216	25.8	2	55.9	25	AAVDTYCR
CAN2	Calpain-2 catalytic subunit	2.4.E-03	483.253	54.0	2	66.6	29	SDTFINLR
STAT1	Signal transducer and activator of transcription 1-α/β	7.3.E-03	486.290	21.7	2	39.1	29	KILENAQR
PRG2	Bone marrow proteoglycan	9.4.E-04	497.742	49.2	2	31.6	27	FQWVDGSR
CXCL7	Platelet basic protein	1.3.E-03	528.761	43.1	2	51.7	28	ICLDPDAPR

line SO-4 (Figure 5D), but not in the non-ATL leukemia cell line Jurkat (Figure 5E). On the other hand, an additional cell proliferation assay using siRNA against *SPTAN1* revealed that reduction of SPTA2 was not sufficient for the induction of cell death for ATL cells (supplemental Figures 3 and 4).

In addition, 3 proteins (PTMS, CH10, and GLYM) were also found to be upregulated in ATL cells. To address the roles of these

proteins, a cell proliferation assay was conducted using 3 ATL cell lines treated with siRNAs against *PTMS*, *HSPE1* (gene symbol of CH10), or *SHMT2* (gene symbol of GLYM) (supplemental Figure 4). As a result, suppression of the *SHMT2* gene induced significant growth inhibition for all 3 ATL cell lines. Although si*HSPE1*-treated KOB cells showed a statistically significant decrease in cell growth rate, si*HSPE1* and si*PTMS* had only partial
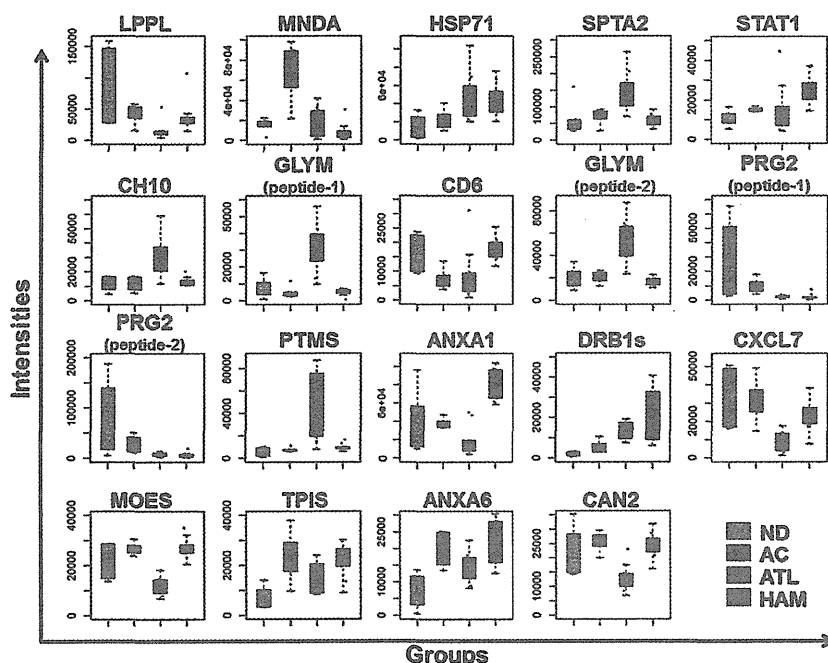

Figure 4. Summary of quantitative features for the 17 protein classifiers identified. The 19 box plots (see Table 1 for protein names) show the results of mass spectrometric quantification and protein identification. We finally identified 19 peptides out of 91 candidates in Figure 3, which were assigned to 17 proteins. Proteins identified from 2 distinct peptides were shown as GLYM (peptides 1 and 2) or PRG2 (peptides 1 and 2). The y-axis indicates normalized relative intensity of peptides in mass spectrometric data. ND, normal donors; AC, asymptomatic carriers.
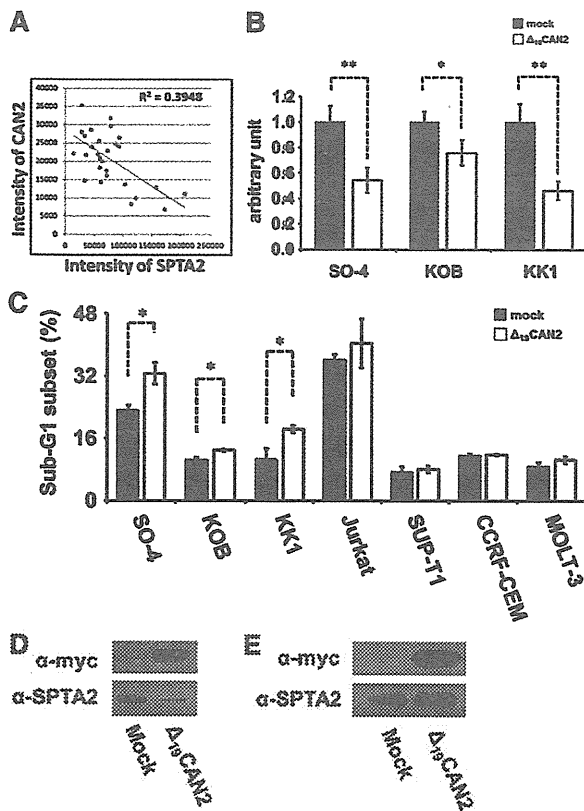
Figure 5. Rescue of CAN2 activity induced cell death in ATL cells. (A) Correlation between CAN2 and SPTA2 expression level in 27 cases. (B) Cell proliferation was measured by MTT assay on SO-4, KOB, and KK1 cells 36 hours after transfection of mock vector or Δ_{19}CAN2. *$P < .05$; **$P < .01$ by Student t test. (C) Overexpression of Δ_{19}CAN2 significantly accelerated cell death in 3 ATL (SO-4, KOB, and KK1) and 4 non-ATL (Jurkat, SUP-T1, CCRF-CEM, and MOLT-3) cell lines. **$P < .05$ by Student t test. The drastic attenuation of SPTA2 expression was observed after transfection of Δ_{19}CAN2 in SO-4 cells (D), but not in Jurkat cells (E). The immunoblot of anti-myc tag confirmed the expression of exogenous Δ_{19}CAN2.

or no effects on proliferation of ATL cell lines. To further confirm whether the overexpression of SPTA2, PTMS, CH10, or GLYM protein would be an ATL-specific molecular signature, the expression levels of these proteins in 8 clinical samples were evaluated by the mass spectrometric quantification technology MRM (supplemental Figures 5 and 6). Expression of SPTA2, GLYM, and CH10 in cells derived from ATL patients was significantly higher than that in cells derived from HAM/TSP patients. The level of PTMS also showed a clearly increasing tendency in the ATL patient group. Taken together, these results suggested that the deprivation of CAN2 activity and upregulation of GLYM in HTLV-1–infected T cells might have a key role at the onset or progression of ATL.

Discussion

In the past decade, proteomics technologies have developed dramatically for the purpose of obtaining more and more comprehensive and sensitive proteome maps in cells or clinical specimens. The performance of mass spectrometers in particular has exhibited remarkable progress; however, as for sensitivity and throughput, it has still been difficult to identify biomarkers from crude samples including body fluids or total cell lysate. A major reason could be

that the range of protein concentration in the analyte is indeed much larger than the dynamic range of recent mass spectrometers.[12] The other essential factor to be improved for clinical proteomics is the capacity of the bioinformatics platform to allow analysis of a sufficient number of clinical samples in order to statistically overcome the significant individual variability.[13]

Concerning the first issue, we previously developed and applied various focused proteomic applications targeting molecular biochemical features including glycan structure biomarkers[14-16] and low-molecular-weight peptide biomarkers.[17] The preenrichment of subproteome fractions effectively reduces the complexity of crude samples and allowed us to identify potential serum cancer biomarkers successfully. Through our previous knowledge, we provide an approach for investigating infectious diseases by employing virus-infected cell-focused proteomics. In addition to HTLV-1, for instance, isolation of HIV-infected cells is highly desired because the frequency of these cells in AIDS patients' PBMCs is ~1 out of 10^4 to 10^5 cells.[18] Actually, we successfully demonstrated the effect of HTLV-1–infected cell isolation on the elimination of individual variability (Figure 2, supplemental Figure 2) and reliable identification of disease state–associated proteins (Figures 4 and 5). We further showed the potential of the next-generation bioinformatics platform Expressionist to remove the constraint on the capacity of data size acquired from high-end mass spectrometers. Expressionist covered whole discovery steps from processing of raw mass spectrometer data to statistical analyses (Figures 1 and 3, and supplemental Figure 1) and, importantly, could perform quantification analysis using a basically unlimited number of clinical samples. Hence, in parallel with the development of mass spectrometers, high-specification and inexpensive OMICS server systems are necessary for future diagnostic marker and therapeutic target discoveries using hundreds or thousands of clinical specimens.

In this study, we focused on the $CD4^+CD25^+CCR4^+$ T-cell subpopulation in which T helper 2, T helper 17, and regulatory T (Treg) cells were mainly involved.[10] The purpose for which we used this subset was to technically enrich the preferential viral reservoir cells and to strengthen reliability of screening results. However, investigating proteome behaviors of these subtypes in HTLV-1–associated diseases is also important physiologically because it has been frequently reported that deregulated Treg plays significant roles in pathogenesis of ATL and HAM/TSP. Indeed, aberrant proliferation of Treg cells is considered the main cause of immunodeficiency in ATL patients because of their innate immunosuppressive functions,[19] whereas abnormal production of interferon γ from infected Treg cells might induce chronic spinal inflammation in HAM/TSP patients.[20] Given the list of our 17 classifier proteins, activation of signal transducer and activator of transcription 1-α/β is the well-known key factor for HAM/TSP,[21] whereas upregulation of heat shock 70-kDa protein 1A/1B, CH10, and PTMS were reported in many other types of tumors.[22-24] The association of these 4 proteins with the etiology of HAM/TSP and ATL would be evident according to the previous work, supporting that our other candidates might similarly have a direct impact on the transformation of Treg cells after infection of HTLV-1. Particularly, the specific upregulation of GLYM in ATL cells represents the first evidence that excessive folate metabolism might be essential for the progression or survival of ATL cells because GLYM is a fundamental enzyme catalyzing the supply of glycine accompanying the conversion of tetrahydrofolate to 5,10-methylenetetrahydrofolate.[25] Indeed, the suppression of GLYM expression, which was confirmed to be upregulated in ATL patients, resulted in significant reduction of cell growth. This observation suggests that diminishing GLYM

expression or enzyme activity could be a promising strategy for molecular-targeting treatment of ATL. Together with the down-regulation of CAN2 in the ATL cells shown in Figure 5, the proteins listed in Table 1 could provide the molecular basis for not only interpretation of physiological mechanisms in ATL or HAM/TSP but also development of novel therapeutic agents for HTLV-1–associated diseases.

CAN2 belongs to a Ca^{2+}-regulated cytosolic cysteine protease family, which includes 14 calpain isoforms.[26] The enzymatic activity of calpain is implicated in diverse physiological processes, such as cytoskeletal remodeling, cellular signaling, and apoptosis.[26] As an example of a spectrin-mediated apoptosis pathway, it was reported that CAN2 produced SPTA2 breakdown products following traumatic brain injury.[27] Because SPTA2 interacts with calmodulin and constructs the membrane cytoskeletons, its breakdown is considered a process of membrane structural changes during cell death.[28,29] This fact is concordant with our finding in ATL, suggesting that accumulation of SPTA2 in ATL cells can be attributed to the suppression of CAN2 expression and contribute to circumvent apoptosis. In the analysis of basal levels of CAN2 and SPTA2 in 7 cell lines (supplemental Figure 7), 3 ATL cell lines showed endogenous expression of CAN2 and moderate levels of SPTA2. On the other hand, 4 non-ATL leukemia cells demonstrated very high expression of SPTA2 and undetectable levels of CAN2. Although we found the downregulation of CAN2 and accumulation of SPTA2 in ATL cells, this tendency might be more distinctive in HTLV-1 (–) leukemia cells. Taken together, even though the expression level of CAN2 was indeed suppressed in ATL cells, the CAN2-SPTA2 apoptotic pathway itself might remain normal. In contrast, this pathway was considered to be impaired at multiple stages in HTLV-1 (–) leukemia cells because CAN2 expression was completely diminished (supplemental Figure 7) and overexpression of CAN2 could not reactivate the CAN2-SPTA2 apoptotic pathway (Figure 5B-E). In these cells, not only genetic downregulation of CAN2 but also inhibition of CAN2 enzymatic activity might be involved in the carcinogenesis.

In conclusion, comprehensive proteomic profiling of HTLV-1–infected T cells provided 17 disease-associated signature proteins, which have great potential for future clinical use as diagnostic biomarkers. As we described regarding the relationship between the CAN2-SPTA2 pathway and ATL phenotypes, further individual functional analyses will contribute to understanding the detailed molecular mechanisms involved in the onset or progression of HAM/TSP and ATL.

Acknowledgments

Authorship

Contribution: M.I. and K.U. designed the study, performed experiments, analyzed results, and wrote the manuscript; A.T. and N.S. performed experiments; N.A., T.S., A.U., and Y.Y. collected the clinical samples and performed flow cytometric experiments; Y.N. and H.N. revised the manuscript; and all authors discussed the results and commented on the manuscript.

Conflict-of-interest disclosure: The authors declare no competing financial interests.

Correspondence: Koji Ueda, Laboratory for Biomarker Development, Center for Genomic Medicine, RIKEN, General Research Building 6F, Institute of Medical Science, 4-6-1 Shirokanedai, Minato-ku, Tokyo, Japan, 1088639; e-mail: k-ueda@riken.jp.

References

1. Yamashita M, Ido E, Miura T, Hayami M. Molecular epidemiology of HTLV-I in the world. J Acquir Immune Defic Syndr Hum Retrovirol. 1996;13(suppl 1):S124-S131.

2. Asquith B, Zhang Y, Mosley AJ, et al. In vivo T lymphocyte dynamics in humans and the impact of human T-lymphotropic virus 1 infection. Proc Natl Acad Sci U S A. 2007;104(19):8035-8040.

3. Sakashita A, Hattori T, Miller CW, et al. Mutations of the p53 gene in adult T-cell leukemia. Blood. 1992;79(2):477-480.

4. Beltran B, Quiñones P, Morales D, Cotrina E, Castillo JJ. Different prognostic factors for survival in acute and lymphomatous adult T-cell leukemia/lymphoma. Leuk Res. 2011;35(3):334-339.

5. Ishida T, Joh T, Uike N, et al. Defucosylated anti-CCR4 monoclonal antibody (KW-0761) for relapsed adult T-cell leukemia-lymphoma: a multicenter phase II study. J Clin Oncol. 2012; 30(8):837-842.

6. Semmes OJ, Cazares LH, Ward MD, et al. Discrete serum protein signatures discriminate between human retrovirus-associated hematologic and neurologic disease. Leukemia. 2005;19(7):1229-1238.

7. Kirk PD, Witkover A, Courtney A, et al. Plasma proteome analysis in HTLV-1-associated myelopathy/tropical spastic paraparesis. Retrovirology. 2011;8:81.

8. Rahman S, Quann K, Pandya D, Singh S, Khan ZK, Jain P. HTLV-1 Tax mediated downregulation of miRNAs associated with chromatin remodeling factors in T cells with stably integrated viral promoter. PLoS ONE. 2012;7(4):e34490.

9. Polakowski N, Gregory H, Mesnard JM, Lemasson I. Expression of a protein involved in bone resorption, Dkk1, is activated by HTLV-1 bZIP factor through its activation domain. Retrovirology. 2010;7:61.

10. Yamano Y, Araya N, Sato T, et al. Abnormally high levels of virus-infected IFN-gamma+ CCR4+ CD4+ CD25+ T cells in a retrovirus-associated neuroinflammatory disorder. PLoS ONE. 2009;4(8):e6517.

11. Oh JH, Gao J, Nandi A, Gurnani P, Knowles L, Schorge J. Diagnosis of early relapse in ovarian cancer using serum proteomic profiling. Genome Inform. 2005;16(2):195-204.

12. Anderson NL, Anderson NG. The human plasma proteome: history, character, and diagnostic prospects. Mol Cell Proteomics. 2002;1(11): 845-867.

13. Nordon IM, Brar R, Hinchliffe RJ, Cockerill G, Thompson MM. Proteomics and pitfalls in the search for potential biomarkers of abdominal aortic aneurysms. Vascular. 2010;18(5):264-268.

14. Ueda K, Katagiri T, Shimada T, et al. Comparative profiling of serum glycoproteome by sequential purification of glycoproteins and 2-nitrobenzensulfenyl (NBS) stable isotope labeling:

a new approach for the novel biomarker discovery for cancer. J Proteome Res. 2007;6(9): 3475-3483.

15. Ueda K, Fukase Y, Katagiri T, et al. Targeted serum glycoproteomics for the discovery of lung cancer-associated glycosylation disorders using lectin-coupled ProteinChip arrays. Proteomics. 2009;9(8):2182-2192.

16. Ueda K, Takami S, Saichi N, et al. Development of serum glycoproteomic profiling technique; simultaneous identification of glycosylation sites and site-specific quantification of glycan structure changes. Mol Cell Proteomics. 2010;9(9): 1819-1828.

17. Ueda K, Saichi N, Takami S, et al. A comprehensive peptidome profiling technology for the identification of early detection biomarkers for lung adenocarcinoma. PLoS ONE. 2011;6(4): e18567.

18. Bahbouhi B, al-Harthi L. Enriching for HIV-infected cells using anti-gp41 antibodies indirectly conjugated to magnetic microbeads. Biotechniques. 2004;36(1): 139-147.

19. Matsubar Y, Hori T, Morita R, Sakaguchi S, Uchiyama T. Delineation of immunoregulatory properties of adult T-cell leukemia cells. Int J Hematol. 2006;84(1):63-69.

20. Best I, López G, Verdonck K, et al. IFN-gamma production in response to Tax 161-233, and frequency of CD4+ Foxp3+ and Lin HLA-